Reconstructing human-environment interactions in the western Messara Plain (Phaistos, Crete, Greece) from the emergence of city states to Byzantine times

Matthieu Ghilardi, Jordi Revelles, Arthur Glais, Tatiana Theodoropoulou, Katerina Theodorakopoulou, Laurent Lespez, Fausto Longo, Amedeo Rossi, Olivier Bellier, Lucilla Benedetti, et al.

Reconstructing human-environment interactions in the western Messara Plain (Phaistos, Crete, Greece) from the emergence of city states to Byzantine times

Matthieu Ghilardi[1], Jordi Revelles[2,3,4], Arthur Glais[5,6,7], Katerina Theodorakopoulou[8], Tatiana Theodoropoulou[9], Laurent Lespez[10,11], Fausto Longo[12], Amedeo Rossi[13], Olivier Bellier[1], Lucilla Benedetti[1], Jules Fleury[1]

Abstract

Landscape evolution from the Early 1st millennium BCE to the mid-1st millennium CE is poorly documented around major archaeological sites in Crete. In a previous publication, the general landscape configuration in the vicinity of ancient Phaistos was reconstructed using a palaeoenvironmental approach, from the Proto-Palatial period (*ca*. 2000 BCE) to the Late-Proto Geometric period (*ca*. 8th cent. BCE). However, the physiography of the landscape, its hydrology and vegetation history remained uncertain for the later archaeological periods. In the present study, additional radiocarbon dates (8) together with pollen, mollusc and sedimentological analyses (CM diagram) were conducted on previously documented sediment cores. These new results enable us to reconstruct in greater detail the landscape history from the Early Archaic period to Late Byzantine times. The results indicate the continuous presence of swampland from the Proto-Geometric period (10th cent. BCE) probably until the initial stages of the Classical period (5th cent. BCE). Subsequently, during the Classical and Hellenistic periods, there was a short interval of alluvial input of terriginous sediments (not exceeding two centuries in duration) which is directly linked with the complete drying up and drainage of the swampland. We address the issue of the possible climatic origin of this abrupt hydrological change, especially in relation to regional climate change and the sedimentary history of adjacent rivers and streams. Tectonic activity in the area is also an important factor and can be invoked as a potential environmental influence. Anthropogenic factors are also considered, even though there is no direct archaeological evidence of drainage in the western Messara Plain during the Archaic and Classical periods. Finally, from Roman times to the Early Byzantine period, floodplain development prevailed in the area and ponds formed locally, in particular from the Late Hellenistic to Early Byzantine periods; this was related to the climatic conditions of the Roman Warm period. Pollen analysis reveals an open forested landscape during the time interval under investigation, within which domesticated plants such as *Olea* (olive) were present. However, the representation of *Olea*

[1]UMR 7330 CEREGE CNRS, Aix-Marseille University, IRD, Collège de France, INRA. Europôle de l'Arbois BP 80 13545 Aix-en-Provence CEDEX 04 – France. ghilardi@cerege.fr
[2]Institut Català de Paleoecologia Humana i Evolució Social (IPHES), Zona Educacional 4, Campus Sescelades URV (Edifici W3), 43007 Tarragona, Spain. jordi.revelles@gmail.com
[3]Universitat Rovira i Virgili (URV), Àrea de Prehistòria, Avinguda de Catalunya 35, 43002 Tarragona, Spain.
[4]Departament de Prehistòria, Universitat Autònoma de Barcelona, 08193 Bellaterra, Spain.
[5]ArScAn Laboratory UMR 7041, MAE, 21 allée de l'université, 92000 Nanterre, arthur.glais@unicaen.fr
[6] LGP UMR 8591. 1 place Aristide Briand, 92195 Meudon CEDEX, France.
[7]Paris 1 University Panthéon-Sorbonne, 75005 Paris, France.
[8]University of Volos, Greece.
[9]University of Côte d'Azur, UMR7264 CEPAM CNRS, Team GReNES, Nice, France
[10]University of Paris Est-Créteil-Val de Marne. Department of Geography. 61, avenue du Général de Gaulle 94010 Créteil, France.
[11]LGP UMR 8591. 1 place Aristide Briand, 92195 Meudon CEDEX, France.
[12]Dipartimento di Scienze del Patrimonio Culturale- University of Salerno - Italy / Phaistos Project flongo@unisa.it
[13]Phaistos Project arossi@unisa.it

decreases continuously from the Late Geometric period to Byzantine times, probably indicating much lower intensity of land use than during Minoan times and possibly also related to the generally colder climatic conditions in Crete from the 8th cent. BCE until the 1st Cent. CE. During this latter interval, there is also the first pollen analytical evidence of *Vitis sp.*

Keywords: Crete; geoarchaeology; paleoenvironments; boreholes; Archaic and Classical periods; Roman and Byzantine times; pollen identification

Research highlights:

- Swamplands around Phaistos lasted until the Classical period (6th-5th Cent. BCE)
- A detrital input is recorded from ca. 450 to 200 cal. BCE
- representation of *Olea* decreases continuously from the Late Geometric period to Byzantine times
- Scarce representation of *Olea* during the Classical period and Byzantine times

1. Introduction

Reconstructing Holocene palaeoenvironments in Crete, the fifth largest Mediterranean island, is a challenging task since continuous sedimentary archives are scarce due to the paucity of permanent lakes and rivers, especially on the southern side of the island. Thus, both the landscape configuration and land-use in Crete, within an archaeological context, remains largely unexplored (Moody, 2000) and little is known about the geomorphological context around the major archaeological sites of the island during Minoan times and later cultural periods from the 1st millennium BCE and CE. In particular, at the end of the Geometric period (8th Cent. BCE), there is the political affirmation represented by independent city states (called *Polis* or *Poleis* in Greek; see, for example: Lefevre-Novaro, 2007); examples are Gortyn and Phaistos (Lefevre-Novaro, 2007; Longo 2015) in the Messara Plain, Priniàs (between Gortyn and Cnossos), Lyttos and Dreros (Eastern Crete), Eleutherna and Axos (in the Rethymno area; Van Effenterre, 1985; Nielsen, 2002). These city states represent a major political, social and economic turning point in the history of Crete, following the demise of the Minoan Kingdom and the so-called "Dark Ages" (see, for example: Lefevre-Novaro, 2007 and 2008). This transition is largely undocumented from a palaeoenvironmental perspective and the effects of anthropogenic activity on landscape configuration and vegetation histories are unclear. Recent attempts to reconstruct both past landuse activities and the agricultural landscape, based on archaeological survey and excavations, have been made (Rossi, 2018) but these are restricted both in time and in space and need to be more documented from a palaeoenvironmental perspective.

The Messara Plain (South Central Crete; Figure 1) hosts several important archaeological sites dating from the Minoan Kingdom until Early Byzantine times (Watrous et al., 2003). It can be considered as one of the most important political and economic centres in the history of Crete. The most important sites include Phaistos (Bredaki et al., 2009) (Figures 1 and 2), one of the former capitals of the Minoan Kingdom, and Gortyn (Figure 1), which was an important city-state from the Geometric to the Hellenistic periods and became the capital of the Province of Crete and Cyrene during Roman times (Francis and Harrison, 2003). The two

major sites of the Western Messara Plain were probably already benefiting from the occurrence of fertile soils during the 2nd half of the 1st millennium BCE.

A palaeoenvironmental research project, conducted at the foot of ancient Phaistos, revealed the existence of a freshwater lake, extant from *ca*. 2000 to 1200-1100 cal. BCE (Ghilardi et al., 2018). Subsequently, after the 3.2 kyr cal. BP Rapid Climate Change (RCC) event, the lake became swampland. This palaeoenvironmental feature had not been documented previously and it was postulated that its investigation by the project might help to elucidate further the archaeology and palaeoeconomy of the area, not only Phaistos, but other sites from the central and western parts of the Messara Plain, such as Gortyn and Aghia Triada. The existence of the palaeo-lake, and adjacent fertile land would have played a major role in the economy and in the socio-political situation in Messara and the surrounding areas, from the late third millennium BCE to the opening centuries of the 1st millennium BCE. The exact timing of the drainage of the swampland remains unclear (though it may have occurred around the 7th Cent. BCE -the early phases of the Archaic period- according to Ghilardi et al., 2018); the subsequent input of detrital sediment has not been dated accurately (though it was dated earlier than the late Hellenistic period according to Ghilardi et al., 2018). Previous palaeofluvial studies conducted in western Messara (of the Gria Saita River; Pope, 2004; Figure 2) have revealed an important phase of sedimentation, probably covering most of the Hellenistic period (300-150 BCE; Pope, 2004). However, the complete history of alluviation has not been documented and there is no information available about the total thickness of these deposits or the coeval fluvial regime. This event was of regional extent and significance, also occurring for example in the Ayiofarango valley (south of the Messara Plain; Figure 1; Doe and Homes, 1977); however, details of the volume of sedimentation and the hydrological history of this former river have not been reconstructed. In addition, the interpretations of both these studies were based solely on the general stratigraphy of a number of different sedimentary profiles that contained reworked Hellenistic pottery sherds in the lower-most parts of the sequences. The chronology of the initial phases of alluviation remain uncertain and further palaeoenvironmental studies are needed to elucidate the fluvial history of Western Messara and the possible role played by the dessication of the palaeo-lake at the foot of ancient Phaistos. Moreover, the synchronous record of alluvial sedimentation during the Hellenistic period had led to questions regarding a possible regional climatic control on fluvial dynamics. Until now, palaeoclimatic reconstructions for Crete have been scarce and reliable data have only been available from other areas of southern Greece, between Crete and the Karpathos Islands (Rohling et al., 2002) and the south central Peloponnesus (Finné et al., 2014; Boyd, 2015).

Based on the palaeoenvironmental study of boreholes, drilled at the foot of ancient Phaistos and previously studied in detail only in their lowermost part (Ghilardi et al., 2018), this paper extends the knowledge base for the region by reconstructing the landscape evolution for the period covering the 1st millennium BCE and the mid-1st millennium CE.

2. Study area and the history of human occupation from the Geometric period to Early Byzantine times.

Located in south central Crete, Messara is the largest plain of the island (Figure 2). It corresponds to an elongated tectonic depression (graben) oriented W/E that has been infilled by clastic sediments during the Neogene and Quaternary (Peterek and Schwarze, 2004; Fytrolakis et al., 2005; Amato et al., 2014). Major fault lines border the Messara depression area to the north and south and are responsible for the steep relief of the Ida and Asteroussia mountain ranges. Several of these major fault lines are reported to be active and could have produced earthquakes during historical times (Monaco and Tortorici, 2004; Mouslopoulou et al., 2011) even if the identification of the potential fault responsible for the destruction of the Minoan palace of Phaistos is still under investigation and the focus of debate (Mouslopoulou et al., 2012). The Aghia Galini, Klima and Aghia Triada fault lines are all located around Phaistos (Fytrolakis et al., 2005; Mouslopoulou et al., 2014; Figure 2) and are invoked to explain the present-day morphology of the area: the archaeological site of Phaistos is located on an uplifted block (horst), called the Phaistos ridge (Fytrolakis et al., 2005; Figure 2) and overhangs the plain to the east. Today, there is no permanent river in the area and the Geropotamos River (Figures 1 and 2) only drains the Messara Plain towards the Tymbaki Gulf, but only during times of high rainfall (mainly spring and autumn). The headwaters of this river mainly drain the Psiloritis mountain range and several of its tributaries, such as the Lethaios River in the area of Gortyn, were especially active during historical times (Bondesan and Mozzi, 2004; Figure 1). Despite major wetland reclamation of the plain, there is some evidence for palaeochannels, in particular at the foot of ancient Phaistos where the bed of the Gria Saita river (dry for most of the year; Figure 2) has deeply incised through floodplain deposits.

The Messara Plain contains two major archaeological sites separated by a distance of *ca*. 12 km: Phaistos was a great Minoan political and economic centre (palatial site) during the 2nd millennium BCE, which subsequently declined during the Early 1st millennium BCE; and Gortyn, which played no major role during Minoan times but was considered as a key settlement in Crete during the 1st millennium BCE and the first centuries of the 1st millennium CE. Today, between these two major archaeological sites, excavated by the Italian School of Archaeology in Greece since the 19th Century CE, fertile land exists, however the character of the landscape was unclear for the 1st millennium BCE and the first half of the 1st millennium CE.

At Phaistos, Protogeometric and Geometric phases (10th-8th centuries BCE) have been recognized on the hill of Christos Effendi (Figure 2), on the Palace hill, and along the eastern slopes (Chalara; Figure 2). The area of Aghia Fotini, on the northern slopes of the Palace hill (Figure 2) – once occupied by Pre-, Proto- and Neopalatial buildings – has yielded burials dated to the Protogeometric and Geometric periods (Rocchetti, 1969-70; Longo, 2015a and 2015b). Other burials, to the southwest of the plateau, indicate that one or more settlement clusters of one of the 90-100 Cretan cities mentioned by Homer were located there (*Il.* II, 649; *Od.* XIX, 172-174). The archaic and classical phases of Phaistos are still poorly documented, apart from the materials unearthed in the area of the Palace and from the settlement of Chalara downhill (Figure 2). The epigraphic documentation (collected in Bredaki *et al.*, 2009, Marginesu, *in press*) and the numismatic evidence (Carbone, 2017 and *in press -1 and 2*-) bear witness, in any case, to the presence of a flourishing community. Only the Hellenistic period (323-150 BCE) can be partly reconstructed on the basis of

excavation records and the interpretation of aerial photographs. Some sectors of the city are known (on the Palace hill, on Christos Effendi, on the plateau, and at Chalara), as well as a numerous wells or cisterns which supplied potable water to houses (Longo, *in press*). The city limits in the Hellenistic period can be deduced by two lines of evidence: on the one hand, from remains of perimeter walls – some already in plain sight, others excavated – northwest of Aghios Ioannis (Figure 2), on the hill of Christos Effendi, and at Chalara; and on the other, by the distribution of burial grounds (Rocchetti, 1969-70; Longo, 2015a; Longo, 2015b; Greco and Betto, 2015; Longo 2017 and Longo, *in press*). There is archaeological evidence that the city was destroyed around the mid 2nd century BCE. This evidence confirms the passage in the work of Strabo (X.4.14) mentioning the occupation of the Phaistian territory by the Gortynians and the end of Phaistos as a city (Bredaki *et al.*, 2009). After a period of abandonment, the hills and the plateau were resettled (2nd-4th century CE; Bredaki and Longo, 2011; Rossi, 2018). An especially important find from the Byzantine phase (from the 5th century CE) is a farm established at Chalara in the 10th century CE, overlying the (barely visible) ruins of earlier buildings.

Gortyn was inhabited by the end of the Neolithic period. The settlement continued in Minoan times, as evidenced by the Minoan farmhouse located in the area of Kannia near the village of Mitropoli, just below Gortyn (Dietrich, 1982; Cucuzza 2011). From the middle of the 1st millennium BCE and thereafter, Gortyn succeeded Phaistos as the dominant power in the Messara Plain. In Hellenistic times, it was one of the largest cities in Crete and the first city to issue a currency on the island. Gortyn needed access to the Libyan Sea, and the nearest port was Lebena or Kaloi Limenes (Figure 2), which was probably under the domination of Phaistos during this period, and also controlled the western part of the Messara Plain and the port of Matala (Perlman, 1995; Figure 1). Therefore, friendly relations with Phaistos were necessary, and perhaps these were achieved via a treaty which was marked by the two cities cutting their first alliance coins (Perlman, 2004; Stefanakis, 1997; Carbone, 2018).

The economic nature of the relationship between the two cities is indicated by a second series of silver coins issued around 380 BCE. Their currencies are the only evidence of their relationship in the second half of the 5th and the beginning of the 4th cent. BCE (Sanders 1982).

3. Climatic conditions in Crete from the Geometric period to Byzantine times: evidence from palaeoenvironmental proxies and contemporary texts

Specific climatic conditions in Crete during the 1st millennium BCE and CE remain uncertain due to the lack of local palaeoclimatic and palaeoenvironmental studies. In particular, there is neither a detailed, well-dated pollen record for this time, nor is there stable isotope evidence from speleothems that can identify local climatic oscillations (including the RCC events reported in Mayewksi et al., 2004 and Finné et al., 2011). However, a marine sediment core drilled NE of Crete, between it and the Karpathos Island (LC21; Rohling et al., 2002; Figure 1), indicates general climatic trends for the southeast Aegean. In addition, two palaeoclimatic records from speleothems (Finné et al., 2014; Boyd, 2015; see Figure 1 for location) have provided significant information for the central and south Peloponnesus (~350 km from central Crete); and local OSL-dated sediment bodies deposited in the Anapodaris (Macklin et

al., 2010; Figure 1) and Istron (Theodorakopoulou et al., 2012; Figure 1) river systems (both situated to the east of the Messara Plain) help us to reconstruct past climatic conditions and to assess their effects on the local fluvial dynamics. Comparison of all of the available records reveals a large degree of intra-regional variability, as previously noted by Finné et al. (2011), which makes comparison between records potentially difficult. However, in Crete, several climatic phases can be identified based on these records and they are described below.

For the 1st millennium BCE, valuable general information is provided by Macklin et al. (2010) who reported a phase of incision in the Anapodaris gorge from *ca*. 3 to 2.07 kyr BP. Their palaeoclimatic interpretation is based on the record of marine core LC21 that indicates increasing sea-surface temperatures in the southeast Aegean during the entire 1st millennium and relatively high $\delta^{18}O$ values in the southeast Mediterranean, reflecting enhanced evaporation and drier conditions in the region. Little is known in detail about the climatic conditions in Crete during the Geometric, Archaic and Classical periods (from the 8th to the 4th Cent. BCE). However, it appears that cold and dry conditions prevailed regionally, with a pronounced peak around the 6th Cent. BCE (Moody, 2016), which is indicated by other studies conducted in central Peloponnesus (Finné et al., 2014; Unkel et al., 2014) and northern Greece (Psomiadis et al., 2017). Concerning flood events, one is clearly reported in the central Peloponnesus around 500 BCE (Finné et al., 2014) and in north central Crete (Kournas Lake) around the mid-5th Cent. BCE (Vannière and Jouffroy-Bapicot, unpublished material cited in Walsh et al., in press). Ancient writers also document the occurrence of human-induced regional floods in the years 418 BCE and 385 BCE caused by the blocking of sinkholes (Finné et al., 2014). Dendrochronological results indicate that growth rings in the 5th century BCE were especially thick compared with previous centuries and the two afterwards (Lamb, 1997). This suggests the occurrence of hotter summers and more rainfall in the 5th century BCE compared with the periods before and after. In Attica, Demosthenes mentions torrential rains, which caused problems for farmers around Eleusis, recalling the winter with heavy rainfall at the beginning of the Peloponnesian War. In addition, Diodoros writes that there were heavy rains in the winter of 427 BCE and that the grain harvest was poor (Sallares, 1991).

During the Hellenistic period (mid-4th-2nd Cent. BCE), climatic conditions in Crete seem to be characterized by a peak in cold and. dry conditions (Moody, 2016), which is also well attested to in the Peloponnesus (Unkel et al., 2014; Finné et al., 2014). An interesting issue concerning the climatic conditions in southern Crete during Hellenistic times is derived from the unique literary source of the 4th Cent. BCE writer Theophrastus in his work "De ventis" (Book II, 47). He reported that, in Crete, "nowadays the winters are more severe and more snowy, resulting in the abandonment of agriculture in most of the plains among the mountains of Ida (situated just north of the Messara Plain) and in the other Cretan mountains..." In earlier times, the mountains there were more fertile, and the island was more populous (e.g. during the Archaic period according to Kardulias and Schutze, 1997); none of the plains were cultivated because they were infertile. Notably, Theophrastus reports that snow lasted on the Ida Mountains for the entire year (HP 4.1.3.). These descriptions of the climate of Crete during the Hellenistic period are in good agreement with a regional palaeoclimatic reconstruction based on palaeoenvironmental proxies (Rohling et al., 2002; Finné et al., 2014; Moody et al., 2016), which indicates cold conditions at the time. Finné et

al. (2014) suggest that wet conditions prevailed in southern Greece during the period 400-100 BCE, as may also have been the case for Crete, according to the description of Theophrastus.

In contrast, Roman times (from approximately the 1st Cent. BCE to the 2nd Cent. CE) are regarded as a warmer and wetter period (Rohling et al., 2002; Moody, 2016) and are known regionally as the 'Roman Optimum' (RO) (Lamb, 1997), also called the 'Roman Warm Period' (Finné et al., 2011; Theodorakopoulou et al., 2012). This climatic event, also recorded elsewhere in the Mediterranean (Lamb, 1997), is characterized by intense sediment deposition at Istron (Eastern Crete) (vertical accretion at the Istron River was around 60-70 cm/cent. during Early Roman times -2nd to 1st Cent. BCE-; Theodorakopoulou et al., 2012). By contrast, in the Anapodaris river system, fine-grained sedimentation, dated to *ca*. 100 CE, suggest minor, low-energy, floods, possibly coupled with changes in land use upstream (Macklin *et al.* 2010). Similar low energy fluvial dynamics with limited sediment accumulation are reported in the Ayiofarango gorge (Doe and Holmes, 1977), located south of the Messara Plain (Figure 1).

Finally, during Late Roman times and the Early Byzantine period (3rd, 4th and 5th Cent. CE), in the south Aegean Sea and in Crete in particular, colder and drier conditions occurred; notably, the 5th Cent. CE can be considered as the peak of aridity on the island (Besonen et al., 2011; Moody, 2016).

In summary, in Crete, the period covering the 1st millennium BCE and the mid-1st millennium CE was characterized by a long phase of cold, arid conditions, only interrupted by the warm and humid conditions of the RO (1st Cent BCE-2nd cent. CE). In general, no major phase of alluvial sedimentation is recorded for the abovementioned period across Crete and only fine-grained sediments, associated with low energy deposition, are recorded with a peak around 100 CE. In the latter case, land use, rather than climate drivers may explain the processes of erosion and deposition.

Only in the Western Messara Plain was there a major input of detrital sediment recorded in the vicinity of Phaistos (Ghilardi et al., 2018); however, this event was not accurately dated and was poorly characterized from a sedimentological perspective. In the present study, we refine the chronology of landscape evolution, erosion and sedimentation patterns to provide a greater understanding of this region.

4. Vegetation of Crete from the Early First Millennium BCE to the mid-1st millennium CE

In Crete, a small number of sites allow the reconstruction of the Holocene vegetation history based on pollen analyses (see Figure 1 for locations). The relevant research has been conducted over the last few decades and mainly focuses on the interval spanning the Neolithic, the Minoan period and the Post-Roman period; there is a hiatus between the post-Minoan period and Roman times. The sampling sites used for vegetation reconstruction are situated near or on the coast as well as inland: e.g., Aghia Galini (South Central Crete; Bottema, 1980; Figure 1), the Akrotiri Peninsula (Moody et al., 1996; Figure 1), Malia (North Central Crete, Lespez et al., 2003; Figure 1) and Palaikastro (Eastern Crete; Cañellas-Boltà et al., 2018; Figure 1). Some of the pollen sequences obtained from inland are from lake environments (see Bottema and Sarpaki, 2003 for Kournas Lake; Figure 1 and Ghosn et al.,

2010 for Omalos pond) in addition to the palaeolake investigated here (western Messara Plain; Ghilardi et al., 2018), and some include peat deposits (Asi Gonia; Atherden and Hall, 1999; Jouffroy-Bapicot et al., 2016; Figure 1). However, despite their geoarchaeological value, few of these studies attempt to reconstruct the vegetation history of Crete from the Early Iron Age to the Byzantine epoch.

The pollen reconstruction of Bottema and Sarpaki (2003) indicates that between 3500 and 1000 BP, around Kournas Lake (North Central Crete; Figure 1) an open, forested landscape was present, dominated by deciduous and evergreen oaks. This study also reveals a decrease in *Olea* (olive) slightly after the Santorini eruption (*ca*. 1630 BCE; however, the chronostratigraphy remains uncertain due to the lack of radiocarbon dating) from *ca*. 20% to less than 5% (Bottema and Sarpaki, 2003). Similarly, in a pollen diagram from Delphinos, *Olea* is poorly represented; it decreases to 6.1% just after the Santorini tephra layer, and finally reaches 2.8% during the 1st millennium BCE (Bottema and Sarpaki, 2003). To explain this phenomenon, Bottema and Sarpaki hypothesize that olive trees were felled after the Santorini eruption because of the reduced demand for olive oil. However, it appears that olive cultivation was still important during Late Minoan times elsewhere in Crete, such as around Phaistos (Ghilardi et al., 2018). Indeed, a pollen sequence obtained in the vicinity of the Minoan Palace (Ghilardi et al., 2018) reveals that *Olea* is highly represented from the 12th Cent. BCE until the 8th Cent. BCE, with percentages ranging generally from 10-40% with highest values (20-45%) during the Late Post-Palatial and Sub-Minoan periods (12th to 11th Cent. BCE). Such high values are only reported in Crete for Late Neolithic and Early Minoan times in the Akrotiri Peninsula (western Crete, Moody et al., 1996), at Istron (central Crete; Theodorakopoulou et al., 2012) and at Palaikastro (eastern Crete; Cañellas-Boltà et al., 2018). Notably, despite the demise of the Minoan Kingdom, *Olea* was still cultivated in the area of Phaistos during the later cultural periods, such as the Proto-Geometric and Geometric (10th-8th Cent. BCE), with a slightly lower representation than during the Late Post-Palatial and Minoan periods (Ghilardi et al., 2018). Nevertheless, the high representation of *Olea* in the vicinity of Phaistos can be explained by its expansion during a period of increasing aridity, corresponding to the 3.2 kyr BP RCC event, and in the context of socio-political instability following the demise of the Minoan Kingdom. Shortly after the early stages of the Geometric period (8th cent. BCE), the representation of *Olea* in the vicinity of Phaistos decreased to a low level (<10%), suggesting a substantial change in the vegetation landscape. However, neither for the Kournas Lake sequence (Bottema and Sarpaki, 2003) nor for the Phaistos sequence (Ghilardi et al., 2018), is a well-dated pollen record available for the period covering the Archaic, Classical and Hellenistic periods.

The only pollen data, with a robust chronostratigraphy and covering the first half of the 1st millennium CE, is from the Asi Gonia peat deposit (north central west Crete; Jouffroy-Bapicot et al., 2016). The pollen record covers the period from early Roman times onward. For the period of 0-300 CE, the vegetation was dominated by *Quercus coccifera*-type (50-80% of TPL) followed by *Erica*-type (up to 30% of the TPL) and *Cistus*-type. Nevertheless, *Olea* is poorly represented (1-5%) with only a single peak at *ca*. 5% around 150 CE (this date also corresponds to the peak of the warm and wet Roman Optimum). A similar situation for *Olea* is reported during the early phases of the Byzantine period. Notably, *Vitis* is not

identified during Roman times, while there is a clear record during early Byzantine times (Jouffroy-Bapicot et al., 2016).

A challenging task is to reveal the vegetation configuration during the time interval from the 8th cent. BCE to the 4th Cent. CE and to evaluate the significance of cultivated species such as *Olea* and *Vitis* within the vegetation record. In general, *Vitis* is barely represented in all pollen sequences obtained in Crete, in particular those spanning Neolithic times to the Late Minoan period.

5. Methods

The boreholes discussed herein are all situated at the foot of ancient Phaistos (Figure 2) with the exact geographic coordinates reported in Ghilardi et al. (2018). For the present study, several cores were reinvestigated, in particular their uppermost stratigraphy (cores Phaistos (Ph) 2, 3, 4, 5, 6 and 9); detailed descriptions of each can be found in Ghilardi et al. (2018).

The new laboratory work comprised mollusc identification for cores Ph 1, 2 and 6 and laser granulometry of the sediments. In total, 148 samples were analyzed using the protocol described in Ghilardi et al. (2008 and 2012). The deposits were classified using two granulometric parameters, the coarsest percentile (C) and the median grain-size (M). These data were extracted from the cumulative grain-size distribution curves following the method of Passega (1957 and 1964) and refined by Bravard and Peiry (1999) for floodplain deposits. C and M for the alluvial deposits are plotted on a log–log scale and the C–M pattern (Fig. 5) is used to evaluate the processes and dynamics of sediment transport and deposition.

Molluscan samples were identified with the help of general atlases for Europe and checklists available for Greece, more specifically Crete (Bank, 2006; Kerney & Cameron, 1999; Locard, 1893; Tachet et al., 2000; Welter-Schultze, 2012). Identification was in most cases pushed to species level.

Pollen samples from cores Ph 2, 3 and 9 were processed following standard methods (Goeury and de Beaulieu, 1979; Girard and Renault-Miskovsky, 1969): treatment with HCL, NaOH, flotation in dense Thoulet liquor, HF and final mounting in glycerine. Pollen grains of terrestrial taxa were identified using an Olympus Bx43 microscope fitted with ×10 oculars and ×40/60 objectives. Hygrophytes (Cyperaceae, *Typha latifolia* and *Typha/Sparganium*) were excluded from the pollen sum to avoid over-representation by local taxa. Due to the poor quality of pollen preservation, only 10 samples provided reliable results and were plotted in a pollen diagram covering the period 1350 cal. BCE to 800 CE (Figure 6), with a focus on the interval ranging from the Archaic period (8th Cent. BCE) to Late Byzantine times (ca. 8th Cent. CE).

In addition, eight new radiocarbon dates (Table 1) from samples of organic matter were obtained from the radiocarbon dating laboratory in Poznan (Poland), with calibration provided by Calib 7.1.0 software (Stuiver and Reimer, 1993; Reimer et al., 2013; Table 1).

6. Results

6.1. Chronostratigraphy and mollusc identification

In Ghilardi et al. (2018), the main sedimentary units and environments for the period from ca. 2000 to 800 cal. BCE were characterized using diatoms and pollens, as well as laser granulometry and magnetic susceptibility analyses. This included the lake sediments of Unit L (identified in the lowermost part of cores Ph 2, 3 (Figure 3) and 9 (Figure 4). In addition, a robust chronostratigraphy was obtained for Unit L (Ghilardi et al., 2018; Figures 3 and 4).

In this study, we use the same cores as described by Ghilardi et al. (2018) in order to provide a more detailed analysis of the sedimentary units in the uppermost part, dated from ca. 800 cal. BCE to 600 cal. CE. The units are described below.

- Unit S1 was identified in cores Ph 2, 3 and 6 (Figure 3). It consisted of gray silty clays with a mollusk assemblage typical of freshwater environments: *Planorbis planorbis, Planorbis corneus, Viviparus viviparus, Oxyloma elegans* and *Myxas glutinosa*. The last species lives mainly in still and clear freshwater in rivers, lakes and swamps. The age of deposition of this swampland sequence ranges from the 10th-9th Cent. BCE (cores Ph 2 and 6) to 537-203 cal. BCE (median probability of 394 cal. BCE; Reimer et al., 2013) in core Ph 2; and 542-381 cal. BCE (median probability of 446 cal. BCE after Stuiver and Reimer, 1993) in core Ph 3. In the uppermost part of Unit S1 in core Ph 6, the mean and modal grain sizes gradually increased: for Unit S1, the mode was generally around 5-10 µm, while in the uppermost part it increased to 30-40 µm, reflecting a detrital input from a source closeby.
- Unit F1 was observed in all cores and was composed of yellow to white heterogeneous material, ranging from fine sands to pebbles. It can be divided in two distinct parts. Sub-Unit F1a consisted of coarse deposits, a mixture of fine to coarse sands with gravels and rounded pebbles, and is only recorded in the lowermost part of cores Ph 4 and 5. Sub-Unit F1b comprised finer deposits (fine to medium yellow sands) which were identified in cores Ph 2, 3, 4 and 6. However, the lack of organic material in F1b prevented the robust dating of this subunit. Nevertheless, the dating of the uppermost part of Unit S1 and the lowermost part of Unit S3 (360-169 cal. BCE) provides an approximate age estimate of ca. 450-400 cal. BCE. Notably, the complete thickness of unit F1 was not recorded and further coring is needed to identify this.
- Unit F2 was recorded in all cores and consisted of coarse silts to fine sands (the mode ranges from 50-100 µm). However, the deposits are not homogeneous and three minor peaks in mean grain-size are evident. The organic matter content was low (2-3%) and the carbonate content was around 20%. Absolute dating of the uppermost part of Unit F2 was only possible for core Ph 3 and 5, where the uppermost part of Unit F2 was dated to 379-285 BCE (core Ph 3) while the lowermost part of unit S3 in core Ph 5 (overlaying unit F2) was dated to 360-169 cal. BCE (median probability of 286 cal. BCE; Stuiver and Reimer, 1993). Combining the radiocarbon dating results for the uppermost part of Units S1 and F2 and the lowermost part of Unit S2 enables the robust dating of Units F1 and F2 (from ca. 450-400 CE to 250-200 BCE). Since Unit F1b was short in cores Ph 2, 3 and 6 (0.2-0.5 m, mainly consisting of fine sands) and directly overlies Unit S1, its age can be estimated at around 450-400 BCE. Unit F2 was about 1.5-2.0-m thick and despite its fine grain size, it was deposited rapidly from ca. 400 to 200 BCE.
- Unit S2 overlay Unit F2 and consisted of gray to white clay. The organic matter content was around 3-5% while the carbonate content was similar to that of Unit S1, generally around 20%. In general, the sedimentological parameters are very similar to Unit

S1. Notably, a peat deposit was recorded in cores Ph 2, 3, 5 and 6 with its thickness ranging from 0.10 m (core Ph 6) to 0.40 m (core Ph 2), indicating a gradually increasing trend from east to west across the Phaistos lowlands. The mollusc identification reveals the presence of freshwater species (the same as described for Unit S1): e.g. *Planorbis planorbis*, *Planorbis corneus*, *Viviparus viviparus* and *Pisidium* sp. (only recorded in the peat deposits). Only *Thebana pisana* (Helicidae) and *Rumina decollata* (Subulinidae), associated with terrestrial environments, are identified in the lowermost part of Unit S1. In core Ph 2, the peat deposit has been accurately dated to between 207-52 cal. BCE (median probability of 153 cal. BCE) for its initial development, and an age of 715-940 cal. CE for its final stages (median probability of 824 cal. CE). The central part of the peat is dated 410-546 CE. Notably, at the base of Unit S2 in core Ph 2, a fragment of mortar (white in colour and 0.20 m thick), was identified. It cannot be linked to any fluvial sedimentation and is likely to be of anthropogenic origin. Between Units F2 and S2, in core Ph 6, colluvium was identified, with a mean grain-size of ~80 µm and a multimodal distribution indicative of poor sorting. This stratum was about 30-cm thick, but is not accurately dated. However, it occurs in the same stratigraphic position as the mortar found in core Ph 2, located 85 m further east. Due to the proximity of the village of Aghios Ioannis, where Hellenistic archaeological structures have been uncovered, this mortar and associated sedimentation may have been anthropogenically influenced. A large piece of charcoal found directly overlying the mortar provides an age estimate of 107 BCE-129 CE, corresponding to early Roman times.

- Unit S3 was only identified in cores Ph 4 and 5. It consisted of white to yellow compact clay with intercalated layers of silt and fine yellow sand. Unit S3 has almost the same sedimentary characteristics as Unit S2. Whilst the basal part of core Ph 5 core has been dated to the Hellenistic period (360-169 cal. BC), no dating was possible of the central and uppermost parts of the unit due to the paucity of organic matter.

6.2. CM diagram

Grain-size classification based on the CM diagram has enabled the identification of five distinct sedimentary deposits (Figure 5), which are described below.

6.2.1. Group (A)

This group is the coarsest, indicating relatively high energy fluvial deposition (M=400-600 µm; C=1230-2000 µm). The sediments were composed of coarse sands and gravels, transported during a phase of high energy floods and probably transported mainly by rolling as bedload. Group A forms a cluster with a distribution parallel to the CM line, indicating that turbulent flow was able to remove the finest sediments in suspension (Passega, 1967; Houbrechts et al., 2013). These detrital sediments are mainly recorded in Unit F1 from cores Ph 4 and 5 and they indicate a former channel of the Gria Saita river.

6.2.2. Group (B)

This group again corresponds to Unit F1 (fluvial sediments) from cores Ph 4 and 5 (belonging to the upper F1b and lower F1a sub-units), both from the central part of the alluvial plain, a short distance from the Gria Saita river. The group is composed of fine to

medium sands, which were transported by rolling and bottom suspension processes (M=140-380 µm; C=1080-1550 µm), indicating transport along the bed of the river.

6.2.3. Groups (C) and (C')

Group (C) is distributed along the CM line, representing varying proportions of the coarse and medium-grained deposits and indicating materials moved in graded suspension (M=50-170 µm; C=150-890 µm). All of the analyzed samples are between 31 and 32 m a.m.s.l. and were present in three cores. The sediments comprise fine and medium sands, mainly from Unit F1 (core Ph 2) and Unit S2 (core Ph 5). They are interpreted as sand bar deposits on the edge of a riverbed, or sheet deposits in a proximal floodplain setting, deposited during a gradual decrease of turbulent flow. The light-gray rectangle, situated above group C, denotes an additional group C', which also shows a parallel trend with groups C and the CM line but which contains coarser particles. These sediments are poorly-sorted and were deposited during a phase of aggradation corresponding to highly turbid flows from an ancient channel of the Gria Saita River, reaching cores Ph 3, 4 and 5 during phases S3 and S2.

6.2.4. Group (D)

This group comprises most of the samples (62 in total) and shows the predominance of a uniform suspension during a long period of alluvial accumulation in the western Messara Plain (M=8-50 µm; C=140-400 µm). The sediments are floodplain sediments representing relatively low flow and turbulent flow velocities. These silty and fine sandy sediments were deposited during the overbank flooding of the Gria Saita River at different times, even though they are mainly composed of sediments from Unit F2, which is the thickest sedimentary layer.

6.2.5. Group (E)

This group is divided into two subgroups (Ea and Eb), which respectively represent sediments with and without the characteristics of decantation processes with additional low energy alluvial inputs: Ea (M=3.5-14 µm; C=48-160 µm) and Eb (M=3.5-10 µm; C=18-60 µm). The sediments of subgroup Ea are present across the entire period of study, while those of subgroup Eb mainly comprise Unit S1. These deposits consist predominantly of samples from cores Ph 2, 3 and 6, and indicate an environment relatively distant from the main channel. The Ea subgroup, recorded in Unit S2 and as topsoil in cores Ph 2, 3 and 6, indicates predominantly low energy deposition with some higher-energy fluvial inputs. However, in core Ph 2, some of the coarsest grains correspond to post-depositional carbonate precipitation (concretions) derived from the progressive illuviation of Unit S2. Subgroup Eb represent decantation deposits lacking fine fluvial sand input and can be interpreted as distal deposits in the ancient lake (Ghilardi et al., 2018).

6.3. Pollen analysis

6.3.1. Core Ph 9

The pollen record from core Ph 9 (Fig. 6a) comes from a phase of limnic clay deposition, dated to Late Minoan times. It provides information about vegetation composition and ecological conditions at a local scale. In most of the samples, NAP were dominant, with high percentages of grassland indicators, mainly Poaceae, with Asteraceae liguliflorae in the lowermost samples (490-550 cm, Figure 6a), and suggesting an open landscape during the whole period. Sclerophyllous taxa predominate amongst the arboreal vegetation, with high values of *Olea* and the presence of *Quercus ilex-coccifera*, *Phillyrea* and *Pinus*, which are characteristic trees in thermo-Mediterranean landscapes. The scarce values of mesic vegetation (only documented in the stratigraphically lowest sample) suggest a phase of dryness during the last centuries of the 2nd millennium BCE. At a local scale there is a clear vegetation change between samples at 490 cm and 470 cm, with the transition from the dominance of Cyperaceae (550-490 cm; *ca*. 1345-1162 cal BCE) to high values of *Typh*a/*Sparganium* (470-430 cm; *ca*. 1102-982 cal BCE). This could be due to changes in water availability, with probable seasonal episodes of desiccation from 490 cm onwards, as shown by the high values of *Pseudoschizaea* (Pantaleón-Cano et al., 1996). The occurrence in these samples of fern spores (monoletes, *Isoetes*, *Ophioglossum*-t, Fig. 6a and type UAB-46) also points to subaerial conditions (Revelles et al., 2016).

6.3.2. Core Ph 3

In core Ph 3, the samples from Unit S1 (520-490 cm; ca. 713-524 cal BCE) yielded reliable pollen spectra. The pollen diagram (Figure 6b) indicates an open landscape (AP around 20-30%) dominated by grassland, mainly with Asteraceae liguliflorae, and with *Olea* and *Pinus* among the tree types. The presence of the pollen of hygrophytes (Cyperaceae and *Typha/Sparganium*) suggests the existence of swampland at the local scale. Nevertheless, the low values of hygrophytes, compared with the results for Ph 2, suggests either a dry phase or that core Ph 3 reflects the signal of a marginal area of the swampland concentrated around Ph 2 (deeper). Decreasing values of *Olea* in Ph 3 (*ca*. 713-524 cal BCE) complete the trend of a decline in *Olea* that started in Ph 2-580 cm (*ca*. 700 cal BCE, Ghilardi et al., 2018) and culminated in Ph 2-178/135 cm (see below).

6.3.3. Core Ph 2

In core Ph 2, only samples from the top part (178-135 cm; ca. 464-797 cal CE) contained reasonably well-preserved pollen (Figure 6c). The samples from 835-520 cm contained very poorly preserved pollen and vegetation reconstruction was not possible for this section. The pollen results from P2 (Figure 6c) show an open landscape (AP values <15-20%). Among the tree pollen types, *Pinus* predominates with *Corylus*, *Quercus ilex-coccifera*, *Olea* and *Pistacia* also represented. The pollen spectra of core Ph 2 indicate grassland, mainly composed of Asteraceae liguliflorae. The existence of swampland at a local scale is attested to by high values of *Typha/Sparganium* and the occurrence of Cyperaceae and *Spirogyra* (freshwater algae). High values of *Pseudoschizaea* suggest episodes of desiccation, which were probably seasonally. The pollen results are consistent with previous studies of this core (section 700-580 cm) (Ghilardi et al., 2018), as in the predominance of Asteraceae and Poaceae and high values of hygrophyte plants.

7. Discussion

7.1. Palaeogeographic reconstruction

The sedimentological data, mollusc identifications, and results of new radiocarbon age estimates presented here allow the palaeogeographic reconstruction of the landscape around ancient Phaistos for the period covering the 8th Cent. BCE until the 6th Cent. CE.

- Previously published results (Ghilardi et al., 2018) revealed that during the Proto-Geometric and Geometric periods, swampland still existed at the foot of Phaistos, in the context of increasing aridity following the 3.2 kyr BP RCC event. In the present study, we dated the uppermost part of the wetland sequence and the radiocarbon dates obtained for cores Ph 2 and 3 reveal ages of 537-203 cal. BCE (2σ) and 542-381 cal. BCE (2σ), respectively. Thus, the last phase of the swampland environment can be reasonably assigned to the 6th and 5th Cent. BCE (Late Archaic to Classical period). The exact spatial extent of the landform feature remains uncertain due to the lack of additional records for boreholes located further east (cores Ph 4 and 5). However, Ghilardi et al. (2018) revealed that 750 m eastward, the swampland (Unit S1 described above) still existed for a short interval after 896-791 cal. BCE, probably until the Classical period. It is likely that the swampland (Unit S1) covered most of the area during the Geometric, Orientalizing, Archaic and Protoclassical periods, close to the course of the modern Gria Saita River.
- During the 5th and 4th Cent. BCE (the Classical period), the input of detrital material is clearly identified in cores Ph 2, 3, 4, 5 and 6 (and it was also identified in the easternmost part of the study area: see Ghilardi et al., 2018). The first stages of this detrital input by fluvial processes is well dated in cores Ph 2 and 3 and clearly corresponds with the Classical period. This phase of deposition did not exceed two centuries, according to the dating of the lowermost part of the swampland unit S3: to 366-166 cal. BCE (from the Late Classical to the Hellenistic period) in core Ph 5, as well as in core Ph 2 where a similar age can be inferred. Sedimentological data clearly indicate that the first phase of this coarse detrital input was associated with high energy processes, probably dating from the 5th Cent. BCE. A second phase of floodplain deposition (overbank alluviaton), dated from the 4th Cent. BCE and characterized the sedimentation pattern across the Phaistos lowlands until the Late Hellenistic period. Finally, the results enable us to date, to the Classical period, the early stages of activity associated with of the Gria Saita River in the lowlands of Phaistos. It is possible that at this time the Gria Saita River was the main drainage artery to the Tymbaki Gulf and can be considered as a palaeochannel and forerunner of the Geropotamos River, which today flows further north (Rossi et al., 2013 and 2018; Amato et al., 2014).

In the nearby Anapodaris catchment, where human occupation was relatively limited during the entire 1st millennium BCE, compared to the western Messara Plain (area of Phaistos), Macklin et al. (2010) only recorded phases of incision with no major episodes of aggradation. Our results clearly differ from the fluvial history of the Anapodaris drainage basin as recorded by Macklin et al. (2010), but they agree well with previous research conducted on the Gria Saita River (Pope, 2004) and in the Ayiofarango valley (Doe and Homes, 1977) that highlight an interval of high energy fluvial activity during the Hellenistic period. This last period corresponds to a peak in cold and dry conditions (Moody, 2016) in the context of increasing temperatures that commenced around the 1st millennium BCE. In

southern Greece this was followed by an abrupt return to wet conditions during the 5th Cent. BCE (Finné et al., 2014). Around Lake Kournas, recent research has indicated a major peak in flooding at ~450 cal. BCE (Vannière and Jouffroy-Bapicot, unpublished data cited in Walsh et al., in press) and it is probably the highest energy event recorded during the entire Holocene (Walsh et al., in press). At ~500 BCE in the Peloponnesus, a flood event is also clearly recorded at Kapsia Cave (Finné et al., 2014) and similar high-energy deposition is observed elsewhere in the central Peloponessus (Unkel et al., 2014).

Following the interval of detrital deposition that started during the Classical period and lasted until the Hellenistic period, there was a new phase of swampland development to the west, together with peat accumulation, which commenced during Early Roman times and lasted until the 8th Cent. CE (confirmed by the high values of *Typha-Sparganium* in Ph 2 from 464-797 cal CE). The peat sequence is only recorded in the cores drilled in the westernmost part of the Phaistos lowlands. In the central part (cores Ph 4 and 5) swamps are affected by occasional detrital input, as confirmed by the granulometry data and the CM diagram. It is probable that due to increased humidity at a local scale, shallow ponds developed. At a regional level, the predominance of sclerophyllous trees among the scarce arboreal vegetation suggests dry Mediterranean climate conditions. The RO, which is characterized by warm and humid conditions starting from the 1st Cent. BCE and lasting until the 2nd to the 3rd Cent. CE, can be invoked to explain peat formation.

During the Early byzantine period, the landscape remained stable and the swampland, its associated peats and other floodplain deposits completely dried out, shaping the subsequent morphology of the Phaistos lowlands. This scenario is in good agreement with the interpretation of Ghilardi et al. (2018) concerning the landscape configuration of the lowlands situated around Phaistos during the last millennium.

7.2. Vegetation history during the Archaic and Classical periods and Late Roman to Early Byzantine times

The pollen results obtained for cores Ph 2, 3 and 9 (Figure 7) reveal an open forested landscape with the predominance of *Olea*, *Pinus* and *Quercus ilex-coccifera* among the arboreal taxa. This predominance of sclerophyllous trees at a regional scale, and the very low percentages of deciduous woodland (*Quercus, Corylus, Carpinus, Alnus* cf. *suaveolens* and *Salix*), suggest a Mediterranean climate with marked seasonality and pronounced summer drought. Ruderal herbs (Poaceae and Asteraceae) are the major component in a highly anthropogenic landscape and, at local scale, hygrophyte communities (Cyperaceae and *Typha/Sparganium*) dominate in phases of shallow lake and freshwater swamp deposition. Despite the lake decline associated with drought conditions during the 3.2 cal ka BP event, swampland would have persisted in the lowlands until the early stages of the 5th century BCE, although there were seasonal droughts as evidenced by high values of fern spores and *Pseudoschizaea*.

The weak representation of *Pinus* indicates its presence at a regional scale, probably in the uplands of the Ida and Asteroussia mountain ranges, rather than in the immediate vicinity of Phaistos. Notably, from *ca*. 700 to 400 cal. BCE, *Olea* representation continuously decreases with a sudden fall around 650-600 cal. BCE. This decrease coincides with a decline

in sclerophyllous trees and a short period of expansion of mesic vegetation, suggesting wetter climatic conditions (Figure 8); this represents the final maximum occurrence of mesic vegetation before the drying up of the swampland due to increasing aridity. Conversely, *Vitis* is represented for the first time ca. 650-600 cal. BCE and it is also identified during the mid-5th cent. BCE, probably reflecting either its cultivation, or perhaps associated with an increase in mesic vegetation (*Vitis vinifera* subsp. *sylvestris* could have developed along riparian environments). Due to the poor pollen preservation in the sediment cores, we have no information about the vegetation composition for the time interval from the Hellenistic period through Roman times. The poor pollen preservation may reflect drier conditions at a local scale, consistent with a cool and dryer climate during the 3rd and 2nd centuries BCE (Moody, 2016). During the Early Byzantine period, the vegetation around Phaistos was dominated by herbs, and a much-reduced forested landscape is attested to by the presence of pine on the slopes of the Ida and Asteroussia mountain ranges. Cultivated plants are scarcely represented at this time: *Olea* was almost absent during the Early Byzantine period, while a low representation of *Vitis* is attested to. The period covering the Early Byzantine period has the lowest percentage of cultivated plants around Phaistos. In northern Crete (the Asi gonia peat bog sequence), the pollen study of Jouffroy-Bapicot et al. (2016) also revealed the very low representation of *Olea* from Roman to Late Byzantine times. Meanwhile, in southern Italy (Apulia, Campania and Sicily), a similar situation was reported with a sharp decrease in *Olea* following a peak around the 1st millennium BCE (Sadori and Narcisi, 2001; Di Rita and Magri, 2009). From ca. 500 BCE to 500 CE, *Olea* is poorly represented in most of the pollen diagrams from southern Italy (Grüger and Thulen, 1998; Di Rita and Magri, 2009) and both climatic (increasing aridity) and anthropogenic factors (selective exploitation and management of wild olive trees for fruit production) may explain the surprisingly low representation of *Olea* during Roman times in southern Italy (Di Rita and Magri, 2009).

In summary, the pollen results for the Phaistos area presented here (Figure 7), together with those of Ghilardi et al. (2018), indicate that *Olea* cultivation was linked to warm and dry climatic conditions, combined with shifts in social and economic strategies. This is because at around the 3.2 kyr BP RCC dry event, *Olea* was dominant in the pollen spectra, with high percentages (10-40%) only recorded during Late Neolithic times and the Early Minoan period elsewhere in Crete. The peak in representation around 3.2-2.8 kyr BP is clearly related to a period of warm, dry conditions (the 3.2 kyr BP RCC event) which favoured the growth of *Olea*. Nevertheless, the high percentages of *Olea* could also be interpreted as the legacy of olive cultivation during former periods (i.e. the Minoan period) and the continuation of favourable climatic conditions maintained the predominance of *Olea* in the landscape. From a social and cultural perspective, this period was characterized by high political instability following the demise of the Minoan kingdom and potential conflicts with the so called Sea People (Cline, 2014). Conversely, during the subsequent periods, ranging from the Early Archaic period to Early Byzantine times, *Olea* is almost absent from our pollen records (Figure 8), as is also the case in northern Crete (Jouffroy Bapicot et al., 2016). This may correspond to a long period of cold and dry conditions in south central Crete. Such conditions are clearly unfavourable for the development of olive cultivation, as it is also suggested for southern Italy (Di Rita and Magri, 2009). Thus, the increasing aridification affecting the

Mediterranean basin during the Late Holocene could have caused the decline of *Olea* in Crete, as well as much of the forest vegetation.

The occurrence of *Vitis* in our pollen records, only attested to after the 8th Cent. BCE (Early Archaic period) and until at least the Early Byzantine period, could reflect its cultivated form, probably imported from the Greek mainland or from elsewhere in Crete, during the Early Archaic period. As was the case for *Olea*, due to unfavourable climatic conditions (cold and dry), vineyard development could have been limited around Phaistos. The presence of *Vitis* may also reflect the riparian form associated with the development of the Gria Saita River, which commenced during Early Archaic times.

7.3. On the possible origin of the alluvial deposition observed during the second half of the 1st millennium BCE (Classical and Hellenistic periods)

The phase of significant detrital input noted in the sedimentological record and dated from the Classical and the early Hellenistic periods could be directly associated with regional climatic change. Indeed, it correlates well with regional alluvial dynamics related to a short phase of intense wet climate that lasted for a maximum of one to two centuries in southern Greece (Kapsia and Alepotrypa caves in Peloponnesus) around the mid-1st millennium BCE (Finné et al., 2011 and 2014; Boyd, 2015; Figure 8). Climate control on river dynamics has been observed elsewhere around Crete, such as in the Peloponnesus during the early stages of the Classical period (Finné et al., 2014; Unkel et al., 2014; Figure 8). Moreover, arguments for a regional climatic control on fluvial dynamics are reinforced by evidence for this alluvial event recorded by multiple rivers (e.g. in the Ayiofarango valley; Doe and Homes, 1977 and the western Messara; Pope et al., 2004; Figure 8) and lake deposits (Vannière and Jouffroy-Bapicot, unpublished material cited in Walsh et al., in press).

A direct human origin of this sudden detrital input cannot be excluded, even if there is neither archaeological of documentary evidence for events. The swampland could have been drained in order to reclaim the area for agriculture and to allow the flourishing settlement of Gortyn to gain access to the Tymbaki Gulf; and in doing so, a river diversion could have been engineered. In the Aegean, there are examples of anthropogenic attempts to modify the courses of rivers: in central south Euboea island, the courses of small streams were diverted and channelized during the 7th Cent. BCE in order to aid the development of the city state of Eretria (Krause, 1985). Indirectly, humans may have changed the catchment hydrology and could be linked to the major changes in land use associated to global climatic cooling in the 1st millennium BCE. Our pollen results, combined with those previously published in Ghilardi et al. (2018), clearly reveal that around Phaistos cultivated plants such as *Olea* were present, within the context of an open forested landscape, from the Late Minoan period to Geometric times (Figures 6a and 8). The climatic conditions of this period are characterized by the 3.2 kyr BP dry event that lasted until ca. 700 BCE with a pronounced peak in aridity observed around 1100 BCE. At the end of Late Geometric times (ca. 700 BCE), colder conditions prevailed and there was an abrupt decrease in the representation of cultivated plants (such as *Olea*, together with only the limited presence of forest taxa; Figure 8). At this time, the slopes were poorly forested and less cultivated, increasing the risk of soil erosion associated with precipitation and runoff. In the Mid-1st millennium BCE there was an abrupt

return to wetter conditions in southern Greece (Finné et al., 2011 and 2014; Figure 8), which triggered intense runoff and erosion around Phaistos and probably within the whole of the western Messara Plain. The development of the Gria Saita River (a possible former course of the Geropotamos R.) was important to landscape evolution and detrital sediment input since it resulted in a short but intense phase of alluviation during a period of wetter climatic conditions around the mid-1st millennium BCE.

Local tectonic activity is another possible cause of the abrupt detrital input. According to Fytrolakis et al. (2005), western Messara is subject to active faulting resulting in violent earthquakes, some of which were recorded during the Prehistorical and historical periods (Monaco and Tortorici, 2004). Several studies conducted along the shoreline of Crete have revealed evidence for uplift related to a number of seismic events (Pirazzoli et al., 1992). One of the most studied seismic events, the "Early Byzantine Tectonic Paroxysm" (EBTP), occurred in *ca*. 365 CE (maximum uplift of 9 m associated with magnitude M>8.5) west of Crete and resulted in the general uplift of western Crete (Pirazzoli et al., 1996). Although detailed and -accurately- dated coastal evidence for this violent seismic event is available (Pirazzoli et al., 1992), until now there was no associated sedimentological or geomorphological evidence for it identified inland. The boreholes drilled in the lowland of Phaistos do not allow us to identify any geomorphological or sedimentological event related to the EBTP, probably because the uplift did not significantly affect the area of Phaistos-Gortyn (Stefanakis, 2010); the landscape was stable during the 4th Cent. CE as evidenced by the presence of ponds containing an undisturbed sedimentary record. The main question is: did an earthquake occur during the Late Archaic to the Classical periods in south central Crete, and if so did it have a major impact on the hydrological configuration of the Messara Plain? Archaeo-seismological evidence of possible mid-1st millennium BCE seismic activity is not reported for the Messara Plain (Ambraseys, 2009). Only Pirazzoli et al. (1992) and Dominey-Howes et al. (1998) report that shoreline uplift occurred at Phalarsana (Western Crete) around 728-358 cal. BCE, but the intensity seems to have been much less than that associated with the EBTP event and would probably not have affected the Messara Plain. In the western Messara Plain, around Phaistos, Monaco and Tortorici (2004) report earthquakes during the Minoan period, while at Gortyn, several seismic events are reported during the Roman and Byzantine periods. Further archaeo-seismological investigations should be conducted in order to identify major earthquakes and to determine whether there was tectonic control upon the hydrological network of the Messara Plain during the 1st millennium BCE.

8. Conclusions

The combined use of different palaeoenvironmental proxies has enabled us to reconstruct the landscape evolution in the vicinity of Phaistos from the Late Geometric period to Byzantine times. Our study is an example of palaeoenvironmental reconstruction for Crete during Ancient Greek and Early Byzantine times, within an archaeological context. The results make clear that swamplands existed in the Phaistos lowlands (western Messara Plain), since at least the late 3rd millennium BCE and dried up around the 5th Cent. BCE. In this study, we have determined the timing of the final drying up phase of the wetlands. We have also identified and precisely dated a large input of coarse detrital material, which contributed to the silting

up of the westernmost part of the Messara Plain during the Classical and Hellenistic periods. A climatic control of this sudden phase of sedimentation, which is associated with fluvial processes around the first millennium BCE, is the most plausible explanation and it is in good agreement with regional fluvial research (conducted to the south of the Messara Plain) and with palaeoclimatic studies conducted in Peloponnesus that reveal major flood events around the 5th-4th Cent. BCE; this followed a period of increasing aridity that started around the 3.2 kyr BP RCC event. However, human intervention, within the cultural context of emerging city states, cannot be excluded as an alternative explanation for this major landscape shift: in order to drain the swamplands and to reclaim the area, a river diversion (anthropogenic forcing) of the Gria Saita could have been undertaken. One of the direct impacts would have been the transformation of the landscape and land-use by the local people from Phaistos. New geoarchaeological perspectives are offered and reinterpretation of the literary sources and inscriptions should be considered in order to elucidate the strongly contrasting economic and socio-cultural evolution of the two sites. This study has for the first time investigated the vegetation composition of Crete from the Late Geometric period to Early Byzantine times, in the vicinity of a major archaeological site, while the period covering the Hellenistic period and Roman times remains little documented. The results indicate that an open forested landscape prevailed with limited land-use: cultivated plants such as *Olea* drastically decreased following the Late Geometric period and were barely present during Greek and Roman times. Conversely, *Vitis* was first identified around Phaistos during Greek and Roman times. The decline of *Olea* can be related to climatic conditions (aridification) observed in Crete from Late Minoan to Early Byzantine times and to major changes in socio-economic strategies during ancient Greek and Roman times.

Acknowledgements

This article is a contribution of the DIKIDA research programme, funded by the ANR (Espace et territoire 2010, ANR-10-ESVS-011-02) and directed by Daniela Lefevre-Novaro (University of Strasbourg, France) for archaeological investigations, and by Matthieu Ghilardi (CNRS, France) for the palaeoenvironmental studies. French National Research Program MISTRALS-PALEOMEX (INEE-INSU; PI: L. Lespez) is also acknowledged for its financial support. The work was made possible by an agreement with the Phaistos Project, a survey programme jointly established between the University of Salerno (Italy) and the Ephoria of Antiquities (Heraklion, Crete, Greece) under the aegis of the Italian Archaeological School in Athens (Greece). Jordi Revelles is a member of the research group GAPS (2017 SGR 836) and acknowledges postdoctoral fellowship support from the Spanish “Juan de la Cierva (FJC2017)” program (MICINN, Spain). The authors also thank two anonymous reviewers for their fruitful comments and Andy Howard for further editorial assistance. Finally, the authors express their deep gratitude to Professor Jan Bloemendal (Univ. of Liverpool, UK) for polishing the English in an earlier version of the article.

References

Amato V., Longo F., Bredaki M., Rossi A., Ghilardi M., Psomiadis D., Colleu M., Sinibaldi L., Delanghe-Sabatier D., Demory F., Petit C., 2014. Geoarchaeological and palaeoenvironmental researches in the area of Ancient Phaistos (Crete, Greece): preliminary results. In Touchais G., Laffineur R., Rougemont F. (eds.), L'environnement naturel et la relation homme-milieu dans le monde égéen protohistorique. Actes du colloque Physis 14, Aegeum Series, 37, 129-140.

Ambraseys, N., 2009. Earthquakes in the Mediterranean and Middle East: a multidisciplinary study of seismicity up to 1900. Cambridge University Press, 968 p.

Atherden, M. A. and Hall, J.A., 1999. Human Impact on Vegetation in the White Mountains of Crete since AD 500. The Holocene, 9, 183–93.

Bank, R.A., 2006. Towards a catalogue and bibliography of the freshwater Mollusca of Greece. Heldia, 6(1/2), 51-86.

Besonen, M.R., Rosenmeier, M.F., Curtis, J.H., Weiss, H., Moody, J.A. and Magill, C.R., 2011. Increasing Evidence for a Pronounced, Mid-1st Millennium AD Desiccation Event in the Eastern Mediterranean. Paper given at AUG Chapman Conference on Climates, Past landscapes, and Civilizations, Santa Fe NM, March 21–25, 2011.

Bondesan, A., Mozzi, P., 2004. Lo studio geomorfologico. In: AA.VV. - Gortyna di Creta, teatro del Pythion, Missione archeologica 2004, Scuola Archeologica Italiana di Atene, Università di Padova, Dipartimento di Scienze dell'Antichità, 17-18.

Bottema, S., 1980. Palynological investigations on Crete. Review of Palaeobotany and Palynology, 31, (1-2), 193-217.

Bottema, S. and Sarpaki, A., 2003. Environmental Change in Crete: A 9000-year Record of Holocene Vegetation History and the Effect of the Santorini Eruption. The Holocene 13, 733–49.

Boyd, M., 2015. Speleothem from Warm Cliamtes-Holocene records from the Caribbean and Mediterranean regions. Phd Thesis, Department of Physical Geography, University of Stockholm, 82 p.

Bravard, J.P., Peiry, J.L., 1999. The CM pattern as a tool for the classification of alluvial suites and floodplains along the river continuum. Geological Society, London. Special Publications 163, 259–268.

Bredaki, M., Longo, F., 2011. Phaistos Survey Project: from the Minoan Palace to the Classical and Hellenistic Town. In I. Gavrlilaki (Ed.), 11th Cretological Congress (Rethymno, 21-27 octobre 2011), Vol. A2.1, Rethymno 2018, 23-43

Bredaki, M., Longo, F., Benzi, M., 2009. Progetto Festòs. Ricognizioni archeologiche di superficie: le campagne 2007-2009.

ASAtene 87(serie III, 9): 935–978.

Cañellas-Boltà, N., Riera-Mora, S., Orengo, H.A., Livarda, A., Knapett, C., 2018. Human management and landscape changes at Palaikastro (Eastern Crete) from the Late Neolithic to the Early Minoan period. Quaternary Science Reviews, 183, 59–75.

Carbone, F., 2017. La monetazione in bronzo di Festòs. In De Caro S., Longo F., Scafuro M., Serritella A. (eds), Percorsi. Scritti di Archeologia di e per Angela Pontrandolfo, II. Paestum, 149-162.

Carbone, F., 2018. Overstriking at Gortyna insights and new perspectives.Proceedings of the 12th International Congress of Cretan Studies, Heraklion, 1-13.

Carbone, F., in press (1). Overstrikes at Phaistos: chronologies and flows", Archaeological Work in Crete 4, Rethymnon.

Carbone, F., in press (2). Rhythms of coin production in III-II century BC: a focus on Gortyna and Phaistos. In Cantilena R., Carbone F. (eds), Monetary and Social Aspects of Hellenistic Crete. Atti del Convegno Internazionale (Atene 13-14 giugno 2018). ASAtene 96, 2018, suppl. 4.

Cline, E.H., 2014. 1177 B.C. The year Civilization collapsed, Princeton University Press, 237 p.

Cucuzza N. 2011, Progetto Kannià: rapporto preliminare sullo studio della Villa minoica in *ASAtene* 87, 2, 2009, 927-933

Di Rita, F., Magri, D., 2009. Holocene drought, deforestation and evergreen vegetation development in the Central Mediterranean: a 5500 year record from Lago Alimni Piccolo, Apulia, southeast Italy. The Holocene, 19 (2), 295-306.

Dietrich, B.C., 1982. Evidence of Minoan religious traditions and their survival in the Mycenaean and Greek world. Historia: Zeitschrift für alte Geschichte, (H. 1), 1-12.

Doe, A.R., Holmes, D.C., 1977. The Physical Environment. In D. Blackman and K. Branigan (eds) An Archaeological Survey of the Lower Catchment of the Ayiofarango Valley Source. ABSA, 72, 13–84.

Dominey-Howes, D., Dawson, A., Smith, D., 1998. Late Holocene coastal tectonics at Falasarna, western Crete: a sedimentary study. Geological Society London Special Publications 146 (1), 343-352.

Finné, M., Bar-Matthews, M., Holmgren, K., Sundqvist, H.S., Liakopoulos, I., Zhang, Q., 2014. Speleothem evidence for late Holocene climate variability and floods in Southern Greece. Quaternary Research, 81, 213-227.

907 Finné, M., Holmgren, K., Sundqvist, H.S., Weiberg, E., Lindblom, M., 2011. Climate in the
908 eastern Mediterranean, and adjacent regions, during the past 6000 years – A review. Journal
909 of Archaeological Science, 38, 12, 3153-3173.
910
911 Francis, J., Harrison G.W.M., 2003. Gortyn: First city of Roman Crete. American Journal of
912 Archaeology, 107 (3), 487-492.
913
914 Fytrolakis, N., Peterek, A. and Schröder, B. 2005. Initial geoarchaeologic Investigations on
915 the Holocene Coastal Configuration near Phaistos/Ayia Triada (Messara Plain, Central Crete,
916 Greece). In: Fouache E and Pavlopoulos K (eds) Sea-Level Changes in Eastern
917 Mediterranean during the Holocene (Zeitschrift für Geomorphologie Suppl. 137). Stuttgart:
918 Schweizebart Science Publishers, 111–123.
919
920 Ghilardi, M., Psomiadis, D., Andrieu-Ponel, V., Colleu, M., Longo, F., Rossi, A., Amato, V.,
921 Gasse, F., Sinibaldi, L., Renard, M., Demory, F., Delanghe, D., Fleury, J., 2018. First
922 evidence of a lake at Ancient Phaistos (Messara Plain, South Central Crete, Greece):
923 reconstructing paleoenvironments and differentiating the roles of human land-use and
924 paleoclimate from Minoan to Roman times. The Holocene, 28, 8, 1225-1244.
925
926 Ghilardi, M., Psomiadis, D., Cordier, S., Delanghe-Sabatier, D., Demory, F., Hamidi, F.,
927 Paraschou, T., Dotsika, E., Fouache, E., 2012. The impact of rapid early- to mid-Holocene
928 palaeoenvironmental changes on Neolithic settlement at Nea Nikomideia, Thessaloniki Plain,
929 Greece. In Ghilardi M. & Tristant Y. (Eds.), Geoarchaeology of Egypt and the
930 Mediterranean: reconstructing Holocene landscapes and human occupation history,
931 Quaternary International, 266, 47-61.
932
933 Ghilardi, M., Kunesch, S., Styllas, M., Fouache, E., 2008. Reconstruction of Mid-Holocene
934 sedimentary environments in the central part of the Thessaloniki Plain (Greece), based on
935 microfaunal identification, magnetic susceptibility and grain-size analyses. Geomorphology,
936 97 (3-4), 617-630.
937
938 Ghosn, D., Vogiatzakis, I. N., Kazakis, G., Dimitriou, E., Moussoulis, E., Maliaka, V. and
939 Zacharias, I., 2010. Ecological Changes in the Highest Temporary Pond of Western Crete
940 (Greece): Past, Present and Future. Hydrobiologia, 648, 3–18.
941
942 Girard, M., Renault-Miskovsky, J., 1969. Nouvelles techniques de préparation en Palynologie
943 appliqués à trois sédiments du Quaternaire final de l'Abri Cornille (Istres -Bouches du
944 Rhône). Bulletin AFEQ, 4, 275-284.
945
946 Goeury, C., de Beaulieu, J.-L., 1979. À propos de la concentration du pollen à l'aide de la
947 liqueur de Thoulet dans les sédiments minéraux. Pollen et Spores XXI (1-2), 239- 251.
948
949 Greco A., Betto A. 2015, Christos Effendi. Archaelogical Studies on the Acropolis of
950 Phaistos: from Minoan to Post-Palatial Age – An INSTAP Project. In P. Karanastasi, A.
951 Tzigiunaki, Ch. Tsigonaki (eds.), Archaeological Works in Crete 3, Rethymno 2015, 483-494
952
953 Grüger, E., Thulin, B., 1998. First results of biostratigraphical investigations of Lago
954 d'Averno near Naples relating to the period 800 BC-800 AD. Quaternary International 47/48,
955 35–40.

Houbrechts, G., Hallot, É., Levecq, Y., Denis, A. C., Van Campenhout, J., Peeters, A., Petit, F., 2013. Images CM de Passega des rivières ardennaises. *Bulletin de la Société géographique de Liège*, *61*, 37-68.

Jouffroy-Bapicot, I., Vannière, B., Iglesias, V., Debret, M., Delarras, J.F., 2016. 2000 Years of Grazing History and the Making of the Cretan Mountain Landscape, Greece. PLoS ONE 11(6): e0156875. https://doi.org/10.1371/journal.pone.0156875

Kardulias, P.N., Shutes, M. T., 1997. Aegean strategies: studies of culture and environment on the European fringe. Rowman & Littlefield.

Kerney, M. P., & Cameron, R. A. D., 1999. A field guide to the landsnails of Britain and North-West Europe. Harper Collins, London.

Krause, C., 1985. Naissance et formation d'une ville. Histoire et archéologie. Les Dossiers 94, 17–25.

Lamb, H.H., 1997. Climate, history and the modern world. 2nd Edition, Routledge, 410 p.

Lefèvre-Novaro, D., 2008. Interactions religieuses entre la Messara (Crète) et la Méditerranée orientale aux XIIe-VIIe s. av. J.-C.. KTÈMA Civilisations de l'Orient, de la Grèce et de Rome antiques, Université de Strasbourg, 33, 259-270.

Lefèvre-Novaro, D., 2007. Les débuts de la polis : l'exemple de Phaistos (Crète). KTÈMA Civilisations de l'Orient, de la Grèce et de Rome antiques, Université de Strasbourg, 32, 467-495.

Lespez, L., Dalongeville, R., Pastre, J.F., Darmon, F., Mathieu, R., Poursoulis, G., 2003. Middle-Late Holocene palaeo-environmental evolution and coastline changes of Malia (Crete). In: Fouache, E. (ed.) The Mediterranean World Environment and History (Collection Environment). Paris: Elsevier, 439–452.

Locard, A., 1893. *Les coquilles des eaux douces et saumâtres de France*. Baillière et fils, Paris.

Longo F. 2015a, Considerazioni preliminary sulla topografia della città greca di Festòs. In Lefevre-Novaro, D., Martzloff, L., Ghilardi, M. Géosciences, Archéologie et Histoire en Crète de l'âge du Bronze Récent à l'époque archaïque, Padova: Ausilio, 159-182

Longo F. 2015b, The Greek Polis in the Light of Recent Topographic Studies. In P. Karanastasi, A. Tzigiunaki, Ch. Tsigonaki (eds.), Archaeological Works in Crete 3, Rethymno 2015, 465-481

Longo, F., 2017, The Fortification Walls of Phaistos: Some Preliminary Conside Annuario della Scuola Archeologica Italiana di Atene e delle missioni italiane in oriente, 95, 497-518.

Longo, F., in press, Nuove prospettive sulle trasformazioni urbane di Festòs. In Cantilena, R., Carbone, F. (eds), Monetary and Social Aspects of Hellenistic Crete. Atti del Convegno

Internazionale (Atene 13-14 giugno 2018). Annuario della Scuola Archeologica Italiana di Atene e delle missioni italiane in oriente 96, suppl. 4.

Macklin, M.G., Tooth, S., Brewer, P.A., Noble, P.L. and Duller, G.A.T., 2010. Holocene Flooding and River Development in a Mediterranean Steepland Catchment: The Anapodaris Gorge, South Central Crete, Greece. Global and Planetary Change 70, 35–52.

Marginesu, G., in press. Le fonti letterarie ed epigrafiche. In: Longo F and Greco A (eds) Festos 1. Athens: Monografie SAIA.

Mayewski, P.A., Rohling, E.E., Stager, J.C., Karlén, W., Maasch, K.A., Meeker, L.D., Meyerson, E.A., Gasse, F., van Kreveld, S., Holmgren, K., Lee-Thorp, J., Rosqvist, G., Rack, F., Staubwasser, M., Schneider, R.R., Steig, E.J., 2004. Holocene climate variability. Quaternary Research 62, 243-255.

Monaco, C., Tortorici, L., 2004. Faulting and effects of earthquakes on Minoan archaeological sites in Crete (Greece), Tectonophysics, 382, 103–116.

Moody, J., 2016. Roman Climate in the Southwest Aegean: Was it really different? In Francis, J., Kouremenos, A. (eds.) Roman Crete: New Perspectives, Chapter 6, Oxford, Oxbow Books, 59-82.

Moody, J., 2000. Holocene climate change in Crete: An archaeologist's view. In: Halstead, P., and Frederick, C., (eds) *Landscape and Land Use in Postglacial Greece* (Sheffield Studies in Aegean Archaeology 3). Sheffield: Sheffield Academic Press, 52–61.

Moody, J., Rackham, O., Rapp, G.Jr., 1996. Environmental Archaeology of Prehistoric NW Crete. Journal of Field Archaeology, 23, 273-297.

Mouslopoulou V., Moreatis D., Fassoulas C., 2011. Identifying past earthquakes on carbonate faults: Advances and limitations of the 'Rare Earth Element' method based on analysis of the Spili Fault, Crete, Greece. Earth and Planetary Science Letters, 309, 45-55.

Mouslopoulou, V., Moreatis, D., Benedetti, L., Guillou, V., Hristopoulos, D., 2012. Is the Spili Fault responsible for double destruction of the Minoan Palace at Phaistos ? John S. Latsis Public Benefit Foundation, Final report, 23 p.

Mouslopoulou, V., Moraetis, D., Benedetti, L., Guillou, V., Bellier, O., Hristopulos, D., 2014. Normal faulting in the forearc of the Hellenic subduction margin: Paleoearthquake history and kinematics of the Spili Fault, Crete, Greece, Journal of Structural Geology, 66, 298-308.

Nielsen, T.H., 2002. Even More Studies in the Ancient Greek Polis (No. 162). Franz Steiner Verlag.

Pantaleón-Cano, J., Perez-Obiol, R., Yll, E.I., Roure, J.M.., 1996. Significado de Pseudoschizaea en secuencias sedimentarias de la vertiente mediterránea de la Península Ibérica e Islas Baleares. Estudios Palinológicos. 101-105.

Passega, R., 1957. Texture as characteristic of clastic deposition. AAPG Bulletin 41, 1952–1984.

Passega, R., 1964. Grain size representation by CM pattern as geological tool. Journal of sedimentary Petrology, 34(4), 830-847.

Perlman, P., 1995. Panhellenic Epangelia and Political Status. Sources for theAncient Greek City-State. Acts of the Copenhagen Polis Centre, 2, 113-64.

Perlman, P 2004. “Crete,” in M.H. Hansen and T.H. Nielsen (eds.), An Inventory of Archaic and Classical Poleis. Oxford, 1144-1195.

Peterek, A., and Schwarze, J., 2004. Architecture and Late Pliocene to recent evolution of outer-arc basins of the Hellenic Subduction Zone (south-central Crete, Greece). Journal of Geodynamics, 38(1), 19–55.

Pirazzoli, P., Laborel, J., Stiros, S.C., 1996. Earthquake clustering in the Eastern Mediterranean during Historical times. Journal of Geophysical Research, 101, 6083-6097.

Pirazzoli, P., Ausseil-Abadie, J., Giresse, P., Hadjidaki, M., Arnold, M., 1992. Historical environmental changes at Phalasarna harbor, West Crete. Geoarchaeology, 7 (4), 371-392.

Pope, K.O., 2004. Geoarchaeology of the Western Mesara. In L. V.Watrous, D. Hadzi-Vallianou and H. Blitzer (eds) The Plain of Phaistos: Cycles of Social Complexity in the Mesara Region of Crete, 39–57. Los Angeles, Monumenta archaeologica 23.

Psomiadis, D., Dotsika, E., Albanakis, K., Galheb, B., Hillaire-Marcel, C., 2018. Speleothem record of climatic changes in the northern Aegean region (Greece) from the Bronze Age to the collapse of the Roman Empire. Palaeogeography, Palaeoclimatology, Palaeoecology, 489, 272-283.

Reimer, P.J., Bard, E., Bayliss, A., Beck, J.W., Blackwell, P.G., Bronk Ramsey, C., Buck, C.E., Cheng., H., Edwards, R.L., Friedrich, M., Grootes, P.M., Guilderson, T.P., Haflidason, H., Hajdas, I., Hatté, C., Heaton, T.J., Hogg, A.G., Hughen, K.A., Kaiser, K.F., Kromer, B., Manning, S.W., Niu, M, Reimer, R.W., Richards, D.A., Scott, E.M., Southon, J.R., Turney, C.S.M., van der Plicht, J., 2013. IntCal13 and MARINE13 radiocarbon age calibration curves 0–50000 years cal. BP. *Radiocarbon* 55(4): 1869–1887

Revelles, J., Burjachs, F. and van Geel, B., 2016. Pollen and non-pollen palynomorphs from the early Neolithic settlement of La Draga (Girona, Spain). *Rev. Palaeobot. Palynol*. 225: 1-20.

Rivière, A., 1977. Méthodes granulométriques-Techniques et interprétations, 170 p.

Rocchetti, L., 1969–1970. Depositi sub-micenei e protogeometrici nei dintorni di Festòs. Annuario della Scuola Archeologica di Atene, 47–48, 41–70.

Rohling, E.J., Mayewski, P.A., Hayes, A., Abu-Zied, R.H. and Casford, J.S.L., 2002. Holocene Atmosphere-Ocean Interactions: Records from Greenland and the Aegean Sea. Climate Dynamics 18, 587–93.

Rossi, A., 2018. Paesaggi della Messarà occidentale tra l'età tardo-ellenistica e l'età romana: topografia, analisi archeomorfologica e nuove prospettive di ricerca. In Annuario della Scuola Archeologica Italiana di Atene e delle missioni italiane in oriente, 96, 118-136.

Rossi, A., Longo, F., Amato, V., 2013. Remote sensing and environmental reconstruction of the site of Phaistos, In: Vermeulen, F., & Corsi, C., (eds.), Non-destructive approaches to complex archaeological sites in Europe: a round-up, RADIO-PAST Radiography of the Past, Ghent Colloquium (15-17 January 2013), 97-98.

Sadori, L., Nacisi, B., 2001. The Postglacial record of environmental history from Lago di Pergusa, Sicily. The Holocene, 11 (6), 655-670.

Sallares, R., 1991. The ecology of the ancient Greek world. Cornell University Press.

Sanders, I.F., 1982. Roman Crete. An Archaeological Survey and Gazetteer of Late Hellenistic, Roman and Early Byzantine Crete. Warminster

Stefanakis, M.I., 1997. Studies in the coinages of Crete with particular reference to Kydonia. University of London (PhD Thesis)

Stefanakis, M.I., 2010. Western Crete: from Colonel Spratt to modern archaeosismology. In: Sintubin, D., Stewart I.S., Niemi T.M., Altunel, E. (eds.) Ancient Earthquakes. Special paper 471, The Geological Society of America, 67-79.

Stuiver, M., Reimer, P.J., 1993. Extended 14C data base and revised CALIB 3.0 14C age calibration program. Radiocarbon 35: 215–230.

Tachet, H., Richoux, Ph., Bournaud, M., Usseglio-Polatera, Ph., 2000. Invertébrés d'eau douce. Systématique, biologie, écologie. Collection « HC Sciences », Éditions CNRS, Paris.

Theodorakopoulou, K., Pavlopoulos, K., Athanassas, K., Zacharias, N., Bassiakos, Y., 2012. Sedimentological response to Holocene climate events in the Istron area, Gulf of Mirabello, NE Crete. Quaternary International, 266, 62–73.

Theodorakopoulou, K., Bassiakos, Y., 2017. Geoarchaeological studies at the cemetery of ancient Kamara, assisted by optically stimulated luminescence (OSL) dating: Insights in the

post-Roman hydrological record of Eastern Crete. Journal of Archaeological Science: Reports 12: 794–804.

Unkel, I., Schimmelmann, A., Shriner, C., Forsén, J., Heymann, C., Brückner, H., 2014. The environmental history of the last 6500 years in the Asea Valley (Peloponnese, Greece) and its linkage to the local archaeological record. Zeitschrift für Geomorphologie, 58 (Suppl. 2), 89-107.

Van Effenterre, H., 1985. La cité; grecque: Des origines à la défaite de Marathon, Hachette, Paris, 339 p.

Walsh K.J., Berger J.F., Roberts N., Vannière B., Ghilardi M., Brown A., Woodbridge J., Lespez L., Estrany J., Glais A., Palmisano A., Finné M., Verstraeten G., in press. The relationship between Holocene demographic fluctuations, climate and erosion in the Mediterranean: a meta-analysis. *The Holocene*, Special issue The changing face of the Mediterranean: land cover, demography and environmental change,

Watrous, L.V., Xatzi-Vallianou D., Pope K. et al., 1993. A survey of the western Mesara plain in Crete: Preliminary report of the 1984, 1986, and 1987 field seasons. Hesperia: The Journal of the American School of Classical Studies at Athens 62(2), 191–248.

Welter-Schultze, F., 2012. European non-marine molluscs. Planet Poster Editions, Göttingen.

Figure and table captions

Figure 1: Location map of the study area and of previous regional palaeoenvironmental investigations. Red stars indicate the location of the main archaeological sites cited in the paper. Yellow squares represent speleothem studies; 1: Kapsia cave (Finné et al., 2014) and 2: Alepotrypa cave (Boyd, 2015). Yellow circles refer to terrestrial records (coring and fluvial stratigraphic profiles): 3: Akrotiri Peninsula (Moody et al., 1996); 4: Kournas Lake (Bottema and Sarpaki, 2003); 5: Asi Gonia peat (Atherden and Hall, 1999; Jouffroy-Bapicot et al., 2016); 6: Malia swamps (Lespez et al., 2003); 7: Istron River (Theodorakopoulou et al., 2012 and 2017); 8: Palaikastro (Cañellas-Boltà et al., 2018); 9: Aghia Galini (Bottema, 1980); 10: Anapodaris River (Macklin et al., 2010). Blue circle refers to marine core: 11 (Rohling et al., 2002). Phai.: Phaistos; Pelopon.: Peloponnesus

Figure 2: Local map of tectonic features and drill corings in the lowland of Phaistos (adapted from Fytrolakis et al., 2005 and Ghilardi et al., 2018). Only cores Ph 2, 3, 4, 5, 6 and 9 were re-analyzed for the present study. Black dash line indicates buried fault line.

Figure 3: Chronostratigraphy of cores Ph 2, 3, 4, 5 and 6. Granulometric parameters and calibrated ages expressed in italics are derived from Ghilardi et al. (2018). Cores Ph 2, 3 and 6 contain 8 unpublished radiocarbon dated samples.

Figure 4: Chronostratigraphy of core Ph 9. In red: section studied for pollen identification for the present paper. See Ghilardi et al. (2018) for further details concerning the full stratigraphic sequence.

Figure 5: CM diagram of late Holocene deposits derived from cores Phaistos 2, 3, 4, 5 and 6. M: median, C: one coarsest percentile

Figure 6: Percentage pollen diagrams established for cores Ph 9 (Fig. 6a), Ph 3 (Fig. 6b) and Ph 2 (Fig. 6c). Values <2% are represented by dots and occurrence of taxa in pollen-poor samples are represented by crosses.

Figure 7: Percentage synthesis pollen diagram based on reliable spectra from cores Phaistos 2, 3 and 9. Values <2% are represented by dots.

Figure 8: Comparison of regional palaeoclimate reconstruction with the sedimentary history of some rivers (that includes the present study) for the last 3000 years in the southern Aegean (Peloponnesus and Crete). Summary of the Holocene palaeoclimate records for: a) South Aegean Sea (relative abundance (%) of Aegean core LC21 planktonic foraminiferal species with warm-water affinities; Rohling et al., 2002) and b) Peloponnesus (b1: δ18O record from Kapsia Cave, central Peloponnesus; Finné et al., 2014 and b2: δ18O record from Alepotrypa Cave, south Peloponnesus; Boyd, 2015); c: Evolution of the vegetation composition for the Mesic and sclerophyllous taxa together with the cultivated plant *Olea* sp. (present study); d: main phases of alluvial aggradation/incision reported for the south Peloponnesus (Finné et al.,

2014), eastern Crete (Theodorakopoulou et al., 2012 and 2017) and south central Crete (Doe and Homes, 1977; Pope et al., 2004; Macklin et al., 2010; the present study).

Table 1: Radiocarbon dating results. * indicates previously published dates in Ghilardi et al., (2018).

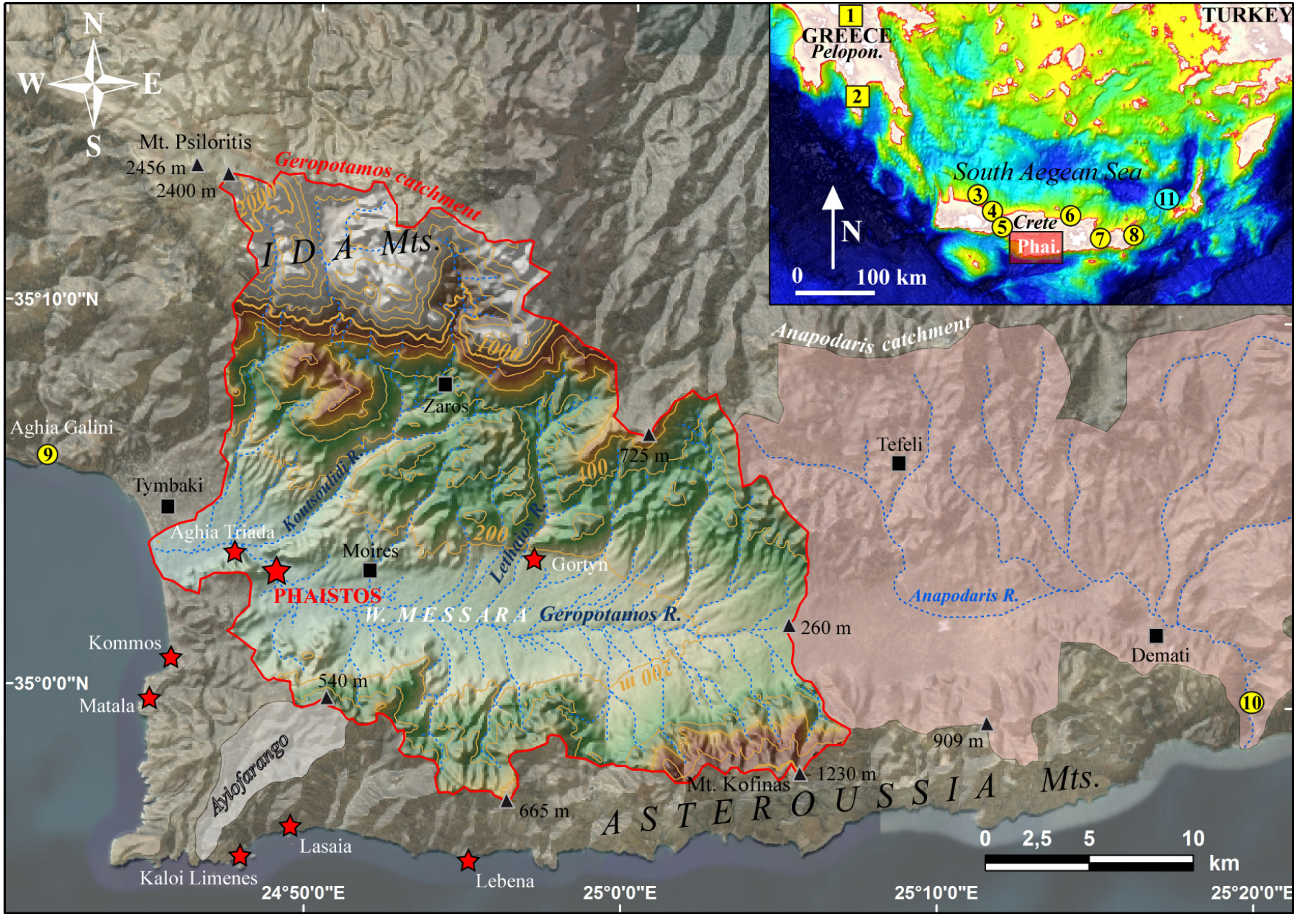
N
W
E
S
Mt. Psiloritis
2456 m
2400 m
Geropotamos catchment
I D A Mts.
-35°10'0"N
Aghia Galini
9
Tymbaki
Aghia Triada
Kamisoutiki R.
Moires
PHAISTOS
Gortyn
Lethaios R.
W. MESSARA
Geropotamos R.
Zaros
725 m
400
200
Kommos
-35°0'0"N
Matala
540 m
Ayiofarango
Lasaia
Kaloi Limenes
Lebena
665 m
24°50'0"E
25°0'0"E
25°10'0"E
25°20'0"E
Anapodaris catchment
Tefeli
Anapodaris R.
260 m
Demati
10
909 m
Mt. Kofinas
1230 m
A S T E R O U S S I A Mts.
0 2,5 5 10
km
1
GREECE
Pelopon.
TURKEY
2
South Aegean Sea
3
4
5
Crete
6
Phai.
7
8
11
N
0 100 km

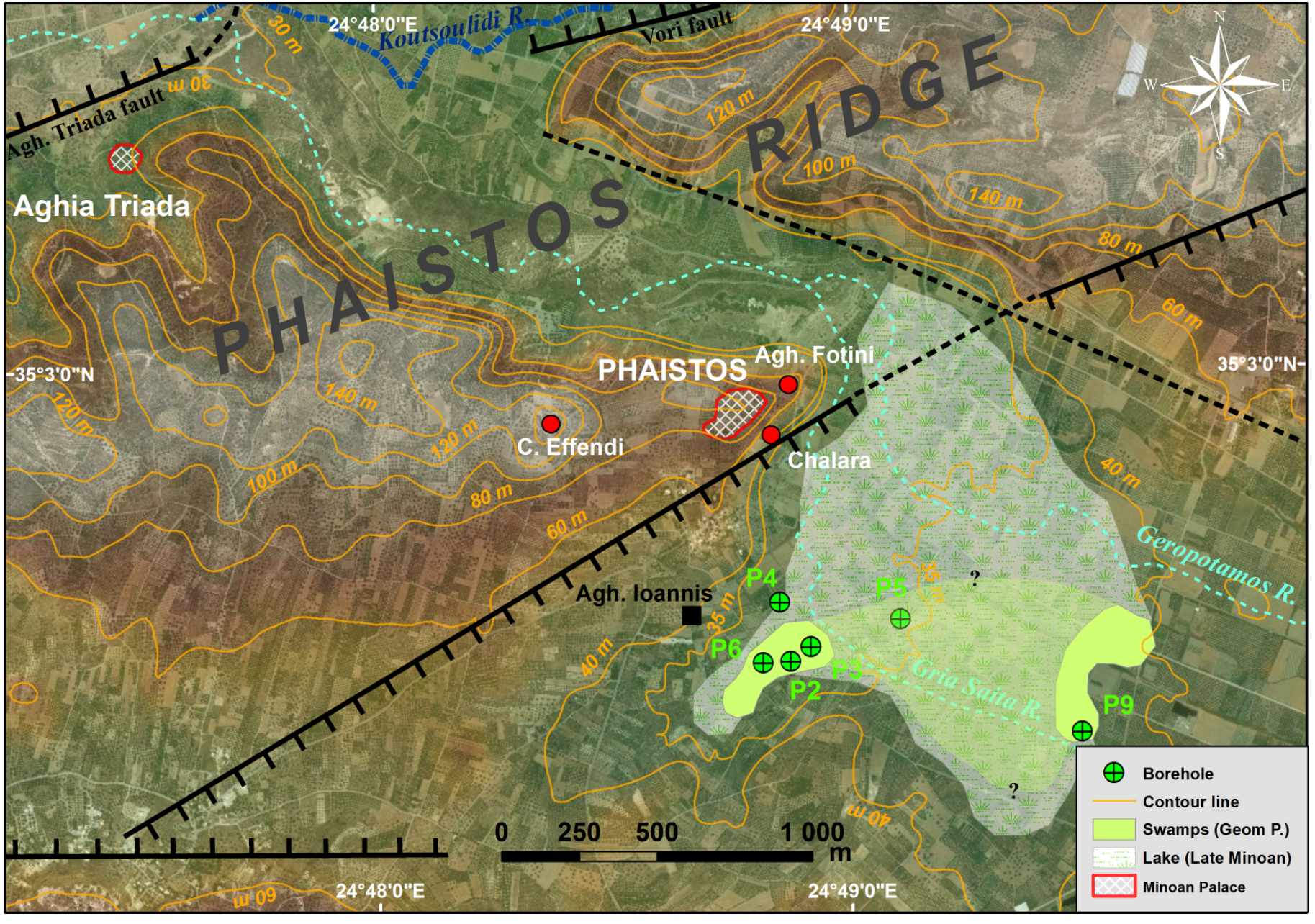
24°48'0"E
Koutsoulidi R.
Vori fault
24°49'0"E
N
W
E
S
Agh. Triada fault
30 m
Aghia Triada
PHAISTOS RIDGE
120 m
100 m
140 m
80 m
60 m
35°3'0"N
PHAISTOS
Agh. Fotini
C. Effendi
Chalara
40 m
Geropotamos R.
Agh. Ioannis
P4
P5
P6
P3
P2
P9
Gria Saita R.
?
0 250 500 1 000
m
Borehole
Contour line
Swamps (Geom P.)
Lake (Late Minoan)
Minoan Palace

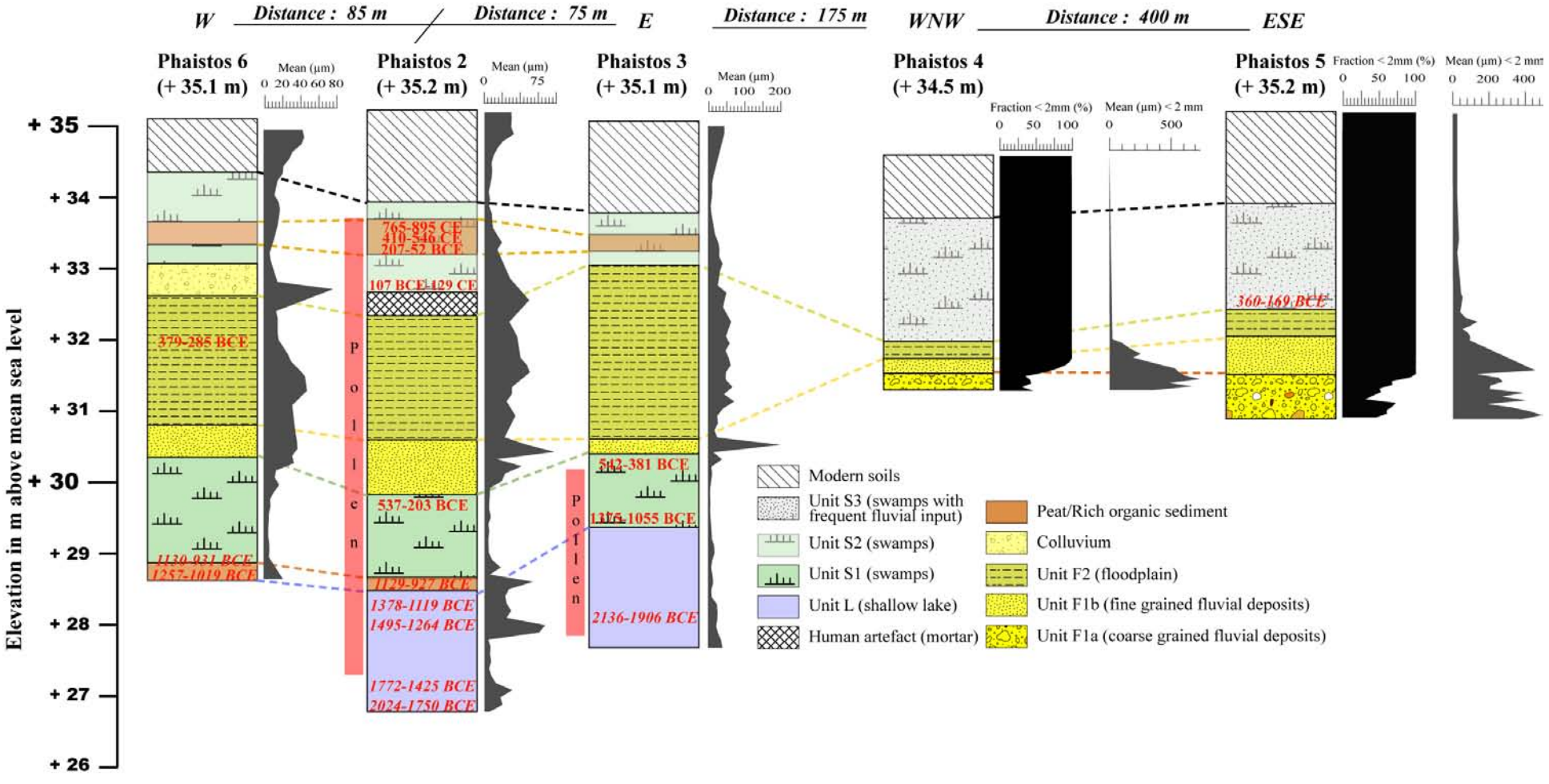
W
Distance : 85 m
Distance : 75 m
E
Distance : 175 m
WNW
Distance : 400 m
ESE
Phaistos 6
(+ 35.1 m)
Phaistos 2
(+ 35.2 m)
Phaistos 3
(+ 35.1 m)
Phaistos 4
(+ 34.5 m)
Phaistos 5
(+ 35.2 m)
Mean (µm)
Fraction < 2mm (%)
Mean (µm) < 2 mm
Elevation in m above mean sea level
+ 35
+ 34
+ 33
+ 32
+ 31
+ 30
+ 29
+ 28
+ 27
+ 26
765-895 CE
410-546 CE
207-52 BCE
107 BCE-129 CE
379-285 BCE
537-203 BCE
1130-931 BCE
1257-1019 BCE
1129-927 BCE
1378-1119 BCE
1495-1264 BCE
1772-1425 BCE
2024-1750 BCE
542-381 BCE
1375-1055 BCE
2136-1906 BCE
360-169 BCE
pollen
Modern soils
Unit S3 (swamps with frequent fluvial input)
Unit S2 (swamps)
Unit S1 (swamps)
Unit L (shallow lake)
Human artefact (mortar)
Peat/Rich organic sediment
Colluvium
Unit F2 (floodplain)
Unit F1b (fine grained fluvial deposits)
Unit F1a (coarse grained fluvial deposits)

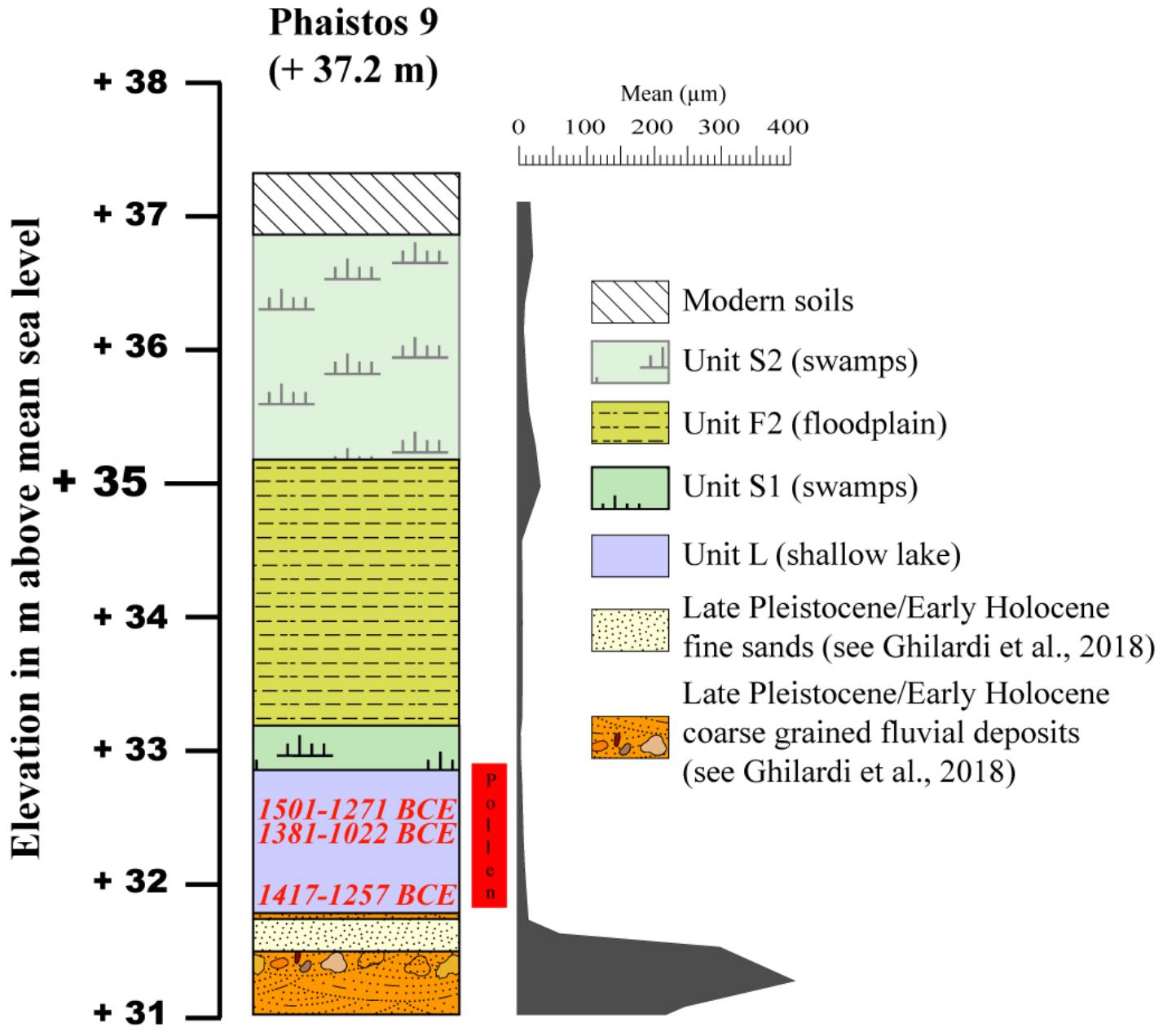
Phaistos 9
(+ 37.2 m)
Elevation in m above mean sea level
+ 38
+ 37
+ 36
+ 35
+ 34
+ 33
+ 32
+ 31
Mean (µm)
0
100
200
300
400
1501-1271 BCE
1381-1022 BCE
1417-1257 BCE
Pollen
Modern soils
Unit S2 (swamps)
Unit F2 (floodplain)
Unit S1 (swamps)
Unit L (shallow lake)
Late Pleistocene/Early Holocene fine sands (see Ghilardi et al., 2018)
Late Pleistocene/Early Holocene coarse grained fluvial deposits (see Ghilardi et al., 2018)

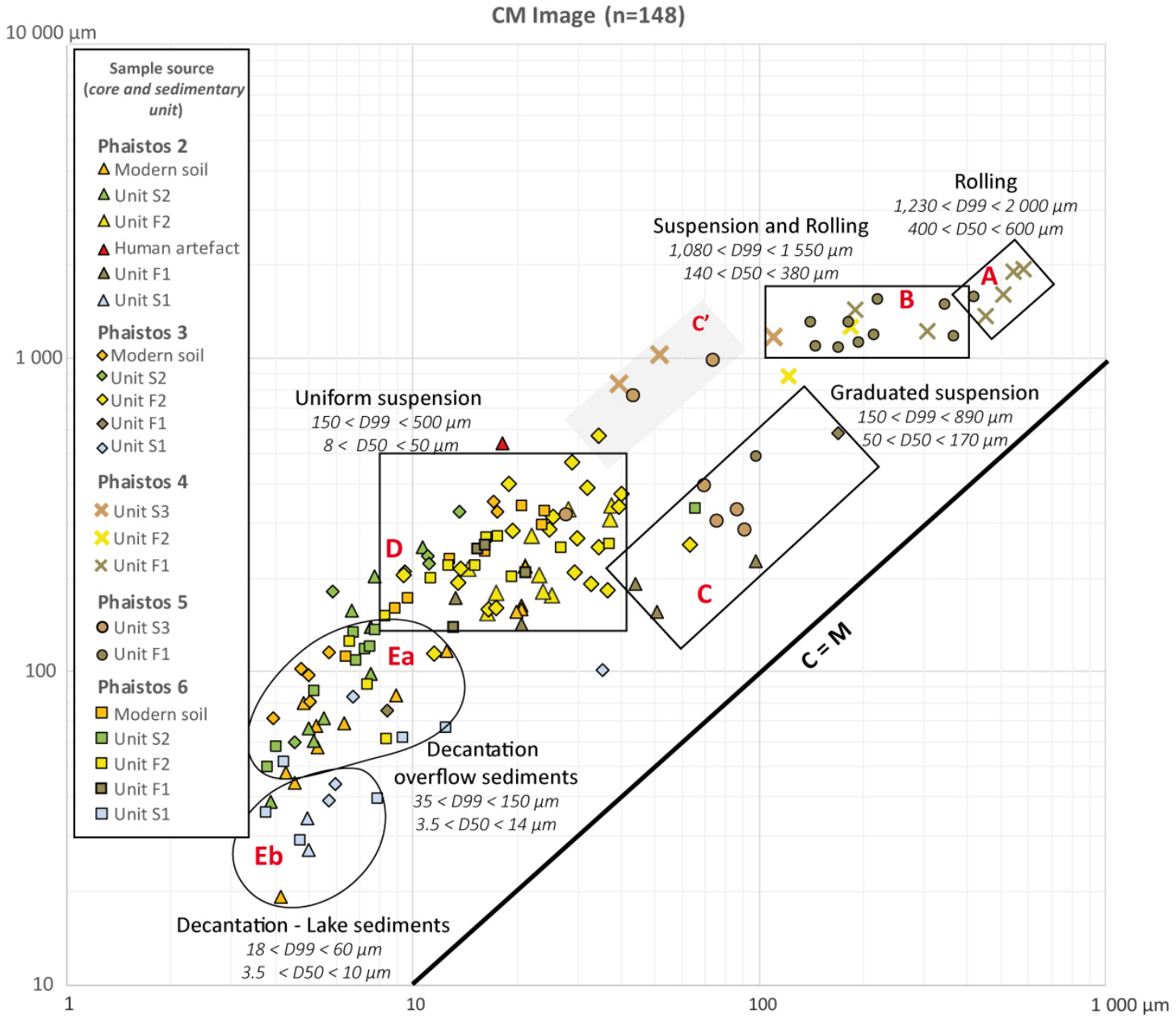
CM Image (n=148)
10 000 µm
1 000
100
10
1
10
100
1 000 µm
Sample source (core and sedimentary unit)
Phaistos 2
Modern soil
Unit S2
Unit F2
Human artefact
Unit F1
Unit S1
Phaistos 3
Modern soil
Unit S2
Unit F2
Unit F1
Unit S1
Phaistos 4
Unit S3
Unit F2
Unit F1
Phaistos 5
Unit S3
Unit F1
Phaistos 6
Modern soil
Unit S2
Unit F2
Unit F1
Unit S1
Rolling
1,230 < D99 < 2 000 µm
400 < D50 < 600 µm
Suspension and Rolling
1,080 < D99 < 1 550 µm
140 < D50 < 380 µm
A
B
C'
Uniform suspension
150 < D99 < 500 µm
8 < D50 < 50 µm
Graduated suspension
150 < D99 < 890 µm
50 < D50 < 170 µm
D
C
Ea
C = M
Decantation overflow sediments
35 < D99 < 150 µm
3.5 < D50 < 14 µm
Eb
Decantation - Lake sediments
18 < D99 < 60 µm
3.5 < D50 < 10 µm

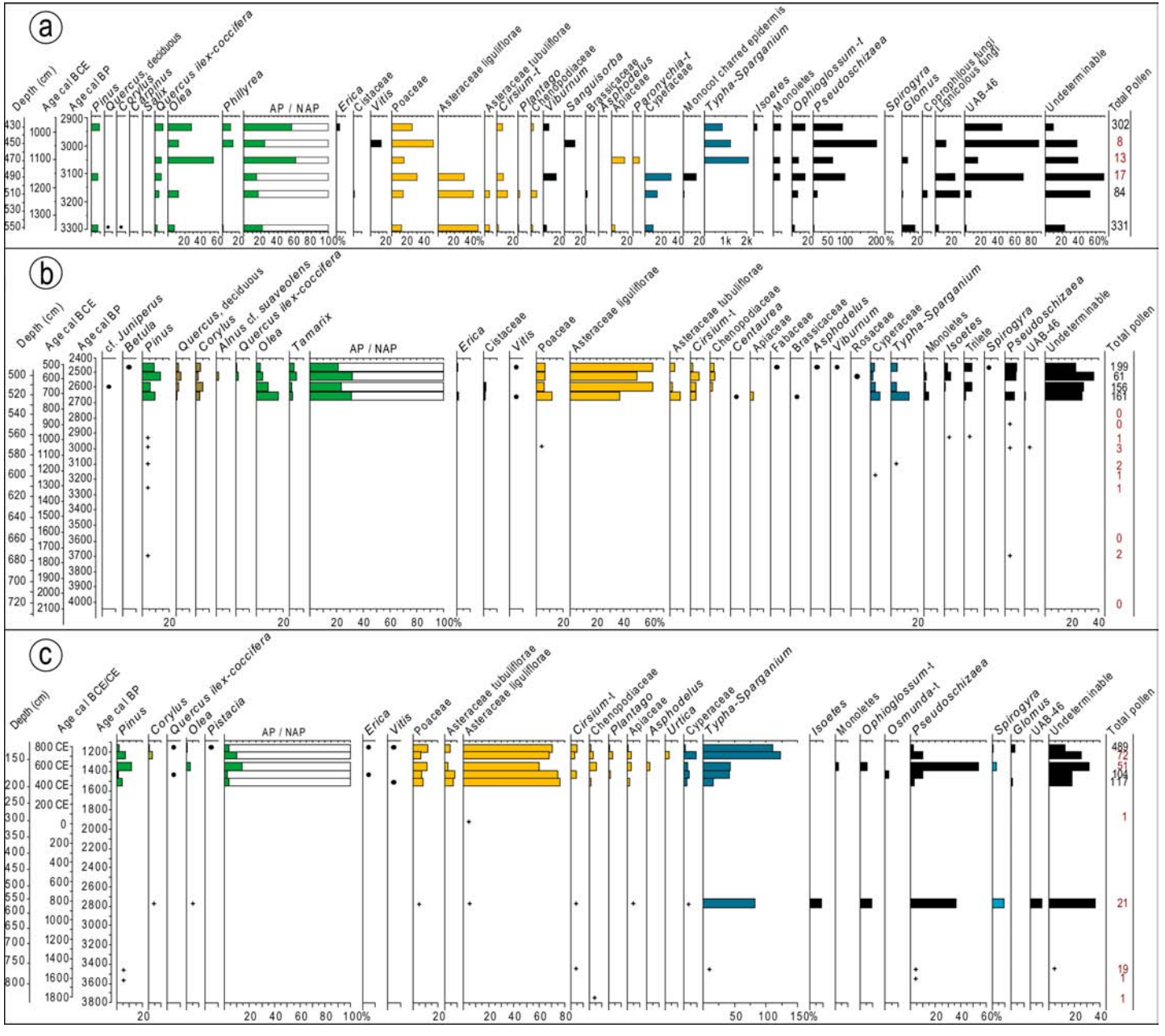
a
Depth (cm)
Age cal BCE
Age cal BP
Pinus
Quercus, deciduous
Corylus
Carpinus
Salix
Quercus ilex-coccifera
Olea
Phillyrea
AP / NAP
Erica
Cistaceae
Vitis
Poaceae
Asteraceae liguliflorae
Asteraceae tubuliflorae
Cirsium-t
Plantago
Chenopodiaceae
Viburnum
Sanguisorba
Brassicaceae
Asphodelus
Apiaceae
Paronychia-t
Cyperaceae
Monocot charred epidermis
Typha-Sparganium
Isoetes
Monoletes
Ophioglossum-t
Pseudoschizaea
Spirogyra
Glomus
Coprophilous fungi
Lignicolous fungi
UAB-46
Undeterminable
Total Pollen
b
Depth (cm)
Age cal BCE
Age cal BP
cf. Juniperus
Betula
Pinus
Quercus, deciduous
Corylus
Alnus cf. suaveolens
Quercus ilex-coccifera
Olea
Tamarix
AP / NAP
Erica
Cistaceae
Vitis
Poaceae
Asteraceae liguliflorae
Asteraceae tubuliflorae
Cirsium-t
Chenopodiaceae
Centaurea
Apiaceae
Fabaceae
Brassicaceae
Asphodelus
Viburnum
Rosaceae
Cyperaceae
Typha-Sparganium
Monoletes
Isoetes
Tilele
Spirogyra
Pseudoschizaea
UAB-46
Undeterminable
Total pollen
c
Depth (cm)
Age cal BCE/CE
Age cal BP
Pinus
Corylus
Quercus ilex-coccifera
Olea
Pistacia
AP / NAP
Erica
Vitis
Poaceae
Asteraceae tubuliflorae
Asteraceae liguliflorae
Cirsium-t
Chenopodiaceae
Plantago
Apiaceae
Asphodelus
Urtica
Cyperaceae
Typha-Sparganium
Isoetes
Monoletes
Ophioglossum-t
Osmunda-t
Pseudoschizaea
Spirogyra
Glomus
UAB-46
Undeterminable
Total pollen

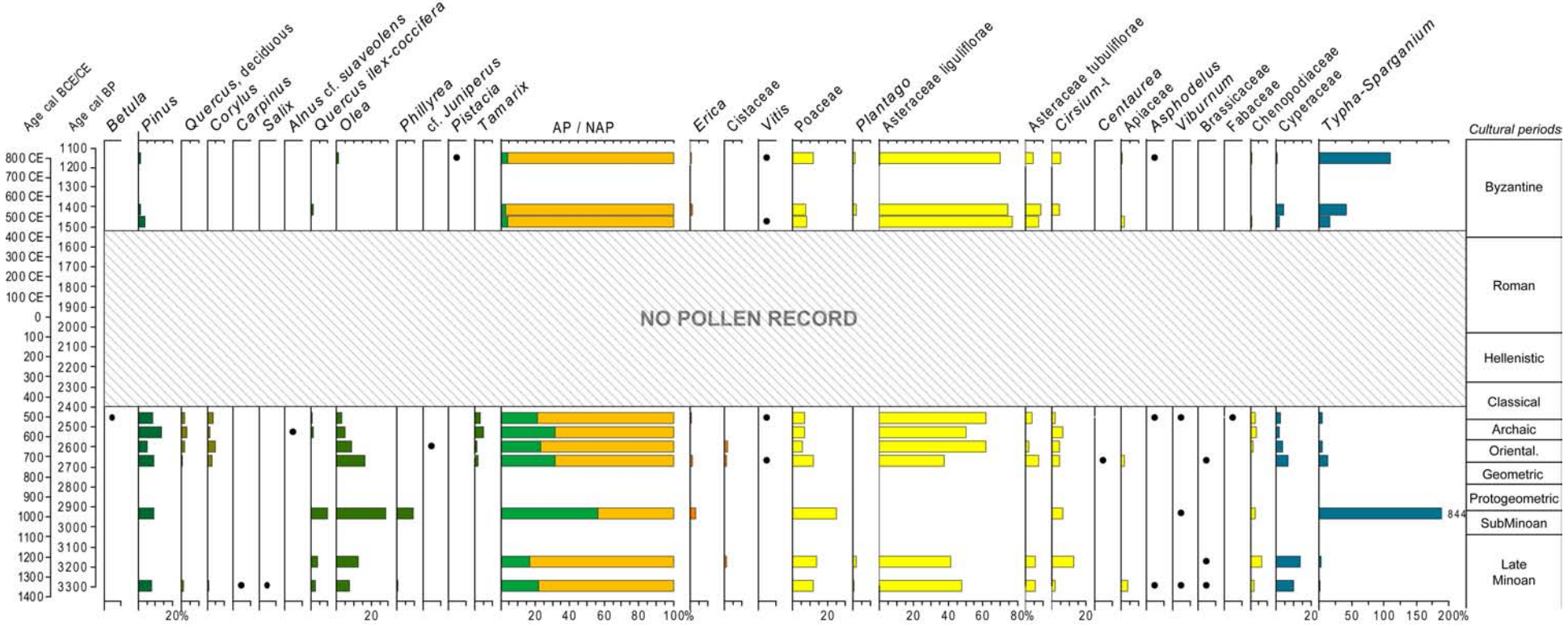
Age cal BCE/CE
Age cal BP
Betula
Pinus
Quercus, deciduous
Corylus
Carpinus
Salix
Alnus cf. suaveolens
Quercus ilex-coccifera
Olea
Phillyrea
cf. Juniperus
Pistacia
Tamarix
AP / NAP
Erica
Cistaceae
Vitis
Poaceae
Plantago
Asteraceae liguliflorae
Asteraceae tubuliflorae
Cirsium-t
Centaurea
Apiaceae
Asphodelus
Viburnum
Brassicaceae
Fabaceae
Chenopodiaceae
Cyperaceae
Typha-Sparganium
Cultural periods
800 CE
700 CE
600 CE
500 CE
400 CE
300 CE
200 CE
100 CE
0
100
200
300
400
500
600
700
800
900
1000
1100
1200
1300
1400
1100
1200
1300
1400
1500
1600
1700
1800
1900
2000
2100
2200
2300
2400
2500
2600
2700
2800
2900
3000
3100
3200
3300
NO POLLEN RECORD
Byzantine
Roman
Hellenistic
Classical
Archaic
Oriental.
Geometric
Protogeometric
SubMinoan
Late Minoan
844
20%
20
20 40 60 80 100%
20
20 40 60 80%
20
20 50 100 150 200%

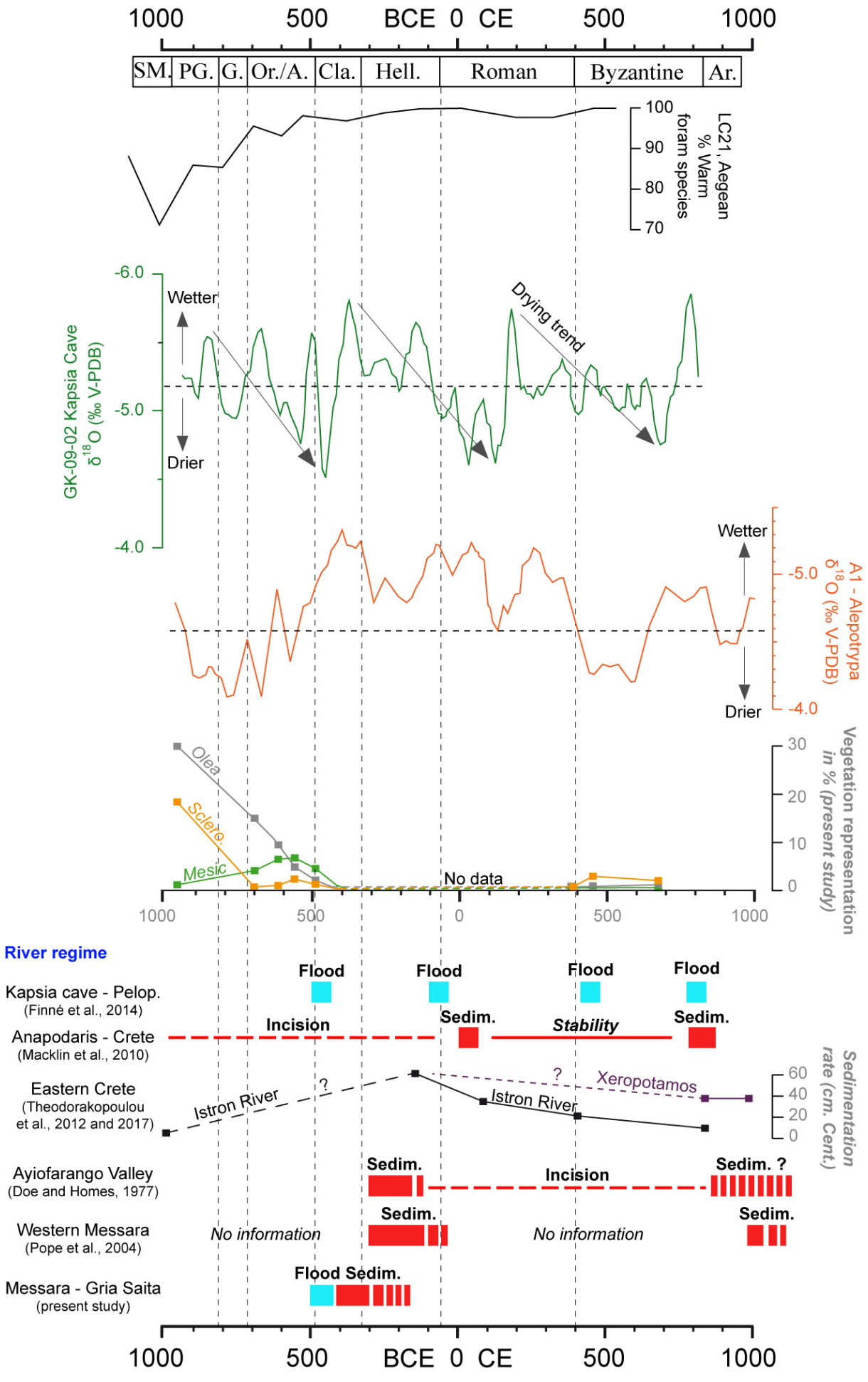
1000
500
BCE 0 CE
500
1000
SM.
PG.
G.
Or./A.
Cla.
Hell.
Roman
Byzantine
Ar.
100
90
80
70
LC21, Aegean
% Warm
foram species
-6.0
-5.0
-4.0
Wetter
Drier
Drying trend
GK-09-02 Kapsia Cave
δ18O (‰ V-PDB)
Wetter
Drier
-5.0
-4.0
A1 - Alepotrypa
δ18O (‰ V-PDB)
Olea
Sclero
Mesic
No data
30
20
10
0
Vegetation representation
in % (present study)
River regime
Kapsia cave - Pelop.
(Finné et al., 2014)
Flood
Flood
Flood
Flood
Anapodaris - Crete
(Macklin et al., 2010)
Incision
Sedim.
Stability
Sedim.
Eastern Crete
(Theodorakopoulou
et al., 2012 and 2017)
Istron River
?
?
Xeropotamos
Istron River
60
40
20
0
Sedimentation
rate (cm. Cent.)
Ayiofarango Valley
(Doe and Homes, 1977)
Sedim.
Incision
Sedim. ?
Western Messara
(Pope et al., 2004)
Sedim.
Sedim.
No information
No information
Messara - Gria Saita
(present study)
Flood Sedim.
1000
500
BCE 0 CE
500
1000

Coring reference	Latitude (WGS 84)	Longitude (WGS84)	Depth (m)	Sample elevation above mean sea level (m)	Material	BP	Error ±	Cal. 2σ	Laboratory reference
Phaistos 2	35°2’38.61’’N	24°48’58.05’’E	1,45	33,72	Peat	1200	30	765-895 CE	Poz-105074
			1,6	33,57	Organic sediment	1580	30	410-546 CE	Poz-110204
			1,75	33,42	Organic sediment	2125	30	207-52 BCE	Poz-103362
			2,57	32,6	Charcoal	1980	50	107 BCE-129 CE	Poz-110205
			5,4	29,77	Charcoal	2310	110	537-203 BCE	Poz-105073
			6,55	28,62	Plant debris	2865	30	1129-927 BCE	Poz-49261*
			7,00	28,17	Plant debris	2990	35	1378-1119 BCE	Poz-49263*
			7,20	27,97	Plant debris	3110	50	1495-1264 BCE	Poz-58147*
			8	27,17	Plant debris	3310	80	1772-1425 BCE	Poz-58104*
			8,40	26,77	Plant debris	3550	50	2024-1750 BCE	Poz-49264*
Phaistos 3	35°2’40.24’’N	24°49’0.63’’E	4,85	30,22	Charcoal	2365	35	542-381 BCE	Poz-102145
			5,93	29,14	Charcoal	2980	40	1375-1055 BCE	Poz-110203
			7,05	28,02	Charcoal	3640	40	2136-1906 BCE	Poz-49266*
Phaistos 5	35°2’42.81’’N	24°49’13.08’’E	2,67	32,58	Charcoal	2180	30	360-169 BCE	Poz-49268*
Phaistos 6	35°2’38.46’’N	24°48’54.82’’E	3,15	31,90	Charcoal	2210	35	379-285 BCE	Poz-110201
			6,20	28,85	Peat	2870	30	1130-931 BCE	Poz-46522*
			6,22	28,83	Peat	2925	30	1257-1019 BCE	Poz-46523*
Phaistos 9	35°2’31.74’’N	24°49’34.37’’E	4,8	28,8	Charcoal	3130	50	1501-1271 BCE	Poz-70961*
			4,94	28,66	Charcoal	2970	50	1381-1022 BCE	Poz-70962*
			5,47	28,13	Charcoal	3070	35	1417-1257 BCE	Poz-73607*